Deep-Sea Research I 101 (2015) 54–70

Contents lists available at ScienceDirect

Deep-Sea Research I

journal homepage: www.elsevier.com/locate/dsri

Long-term (1993–2013) changes in macrozooplankton off the Western Antarctic Peninsula

Deborah K. Steinberg [a,*], Kate E. Ruck [a], Miram R. Gleiber [a], Lori M. Garzio [a], Joseph S. Cope [a], Kim S. Bernard [b], Sharon E. Stammerjohn [c], Oscar M.E. Schofield [d], Langdon B. Quetin [e], Robin M. Ross [e]

[a] Virginia Institute of Marine Science, College of William & Mary, Gloucester Pt., VA 23062, USA
[b] College of Earth, Ocean, and Atmospheric Sciences, Oregon State University, Corvallis, OR 97331, USA
[c] Institute of Arctic and Alpine Studies, University of Colorado at Boulder, Boulder, CO 80309, USA
[d] Institute of Marine and Coastal Sciences, Rutgers University, New Brunswick, NJ 08901, USA
[e] Marine Science Institute, University of California at Santa Barbara, Santa Barbara, CA 93106, USA

ARTICLE INFO

Article history:
Received 19 September 2014
Received in revised form
6 February 2015
Accepted 6 February 2015
Available online 9 March 2015

keywords:
Southern Ocean
Krill
Zooplankton
Climate
Sea ice

ABSTRACT

The Western Antarctic Peninsula (WAP) is one of the most rapidly warming regions on Earth, and where a high apex predator biomass is supported in large part by macrozooplankton. We examined trends in summer (January–February) abundance of major taxa of macrozooplankton along the WAP over two decades (1993–2013) and their relationship with environmental parameters (sea ice, atmospheric climate indices, sea surface temperature, and phytoplankton biomass and productivity). Macrozooplankton were collected from the top 120 m of the water column in a mid-Peninsula study region divided into latitudinal (North, South, and Far South) and cross-shelf (coastal, shelf, slope) sub-regions. Trends for krill species included a 5-year cycle in abundance peaks (positive anomalies) for *Euphausia superba*, but no directional long-term trend, and an increase in *Thysanoessa macrura* in the North; variability in both species was strongly influenced by primary production 2-years prior. *E. crystallorophias* abundance was best explained by the Southern Annular Mode (SAM) and Multivariate El Niño Southern Oscillation Index (MEI), and was more abundant in higher ice conditions. The salp *Salpa thompsoni* and thecosome pteropod *Limacina helicina* cycled between negative and positive anomalies in the North, but showed increasing positive anomalies in the South over time. Variation in salp and pteropod abundance was best explained by SAM and the MEI, respectively, and both species were more abundant in lower ice conditions. There was a long-term increase in some carnivorous gelatinous zooplankton (polychaete worm *Tomopteris* spp.) and amphipods. Abundance of *Pseudosagitta* spp. chaetognaths was closely related to SAM, with higher abundance tied to lower ice conditions. Long-term changes and sub-decadal cycles of WAP macrozooplankton community composition may affect energy transfer to higher trophic levels, and alter biogeochemical cycling in this seasonally productive and sensitive polar ecosystem.

1. Introduction

The Western Antarctic Peninsula (WAP) is a highly productive region of the Southern Ocean, supporting a high biomass of krill (Atkinson et al., 2009) and higher-level consumers such as penguins, seals, and whales (Smetacek and Nicol, 2005; Nowacek et al., 2011). The WAP region has undergone considerable change and rapid warming, with an increase in winter air temperatures of 6 °C from 1950–2001 (Vaughan et al., 2003), and increases in sea surface temperature, ocean heat content, and wind (Meredith and King, 2005; Martinson et al., 2008; Holland and Kwok, 2012). These changes are coupled to a rapidly shortening annual sea ice season caused by an earlier spring sea ice retreat and a later autumn sea ice advance (Stammerjohn et al., 2008a, 2012). A consequence of this regional warming is that a latitudinal climate gradient exists along the length of the WAP, with a warmer, moist, maritime climate in the north, and a colder, drier, continental climate in the south (Smith et al., 1999; Ducklow et al., 2012a, 2012b, 2013). A manifestation of this gradient is that the northern WAP near Palmer Station on Anvers Island is presently nearly ice-free (sea ice season duration ~3.5 months), while in the south (Marguerite Bay southward) perennial sea ice still persists (~7.5 months) – although sea ice has decreased in extent and duration throughout the WAP over time (Ducklow et al., 2013).

* Corresponding author.
E-mail address: debbies@vims.edu (D.K. Steinberg).

http://dx.doi.org/10.1016/j.dsr.2015.02.009
0967-0637/

These environmental changes are affecting the WAP marine pelagic ecosystem differently along a north to south gradient. In the far northern WAP (tip of Peninsula to Anvers Island), the increase in winds and clouds, juxtaposed on a longer open water season has led to deeper mixed layers and more variable light conditions, resulting in decreased phytoplankton (chlorophyll *a*) biomass (Montes-Hugo et al., 2009) and shifts from larger diatoms to smaller flagellates (Montes-Hugo et al., 2010), compared to the south. Recent north vs. south comparisons within the Palmer Long Term Ecological Research (PAL LTER) mid-WAP study region also indicate smaller and less abundant microzooplankton in the north (Garzio and Steinberg, 2013), and lower lipid content and thus food quality of Antarctic krill (*Euphausia superba*) in the north (Ruck et al., 2014). There are distinct regional (Ross et al., 2008, 2014; Parker et al., 2011) and interannual (Ross et al., 2008, 2014) patterns of abundance in the major taxa of macrozooplankton in the mid-WAP. These differences in turn affect the relative impact of various macrozooplankton grazers, as illustrated in a two-year study showing shifts from dominant grazing by krill and pteropods in the south, to salps in the north (Bernard et al., 2012), and is suggested as a mechanism affecting WAP phytoplankton community composition (Garibotti et al., 2003). Long-term changes in the WAP food web, as characterized by an inverse model approach, indicate the north WAP is characterized by an increasingly dominant role of the microbial loop (as opposed to krill) in food web carbon flow, while in the south there is no detectable long-term trend toward dominance of either a microbial- or a krill-based food web (Sailley et al., 2013).

Both long-term (i.e., >10 years) changes in macrozooplankton abundance attributed to warming, and sub-decadal-scale shifts attributed to oscillations in atmospheric forcing, have been documented in the Antarctic Peninsula region. A long-term shift from a dominance of the Antarctic krill, *Euphausia superba*, to salps (mainly *Salpa thompsoni*) occurred in the SW Atlantic sector of the Southern Ocean during the period 1926–2003 (Atkinson et al., 2004). In the Elephant Island region just north of the Peninsula, a decline in sea ice during the period 1976–1996 was significantly correlated with a decrease in Antarctic krill and an increase in salps. In the WAP there was an increase in the range and frequency of occurrence of salps over the period 1993–2008 (Ross et al., 2008, 2014), with a negative correlation between salp abundance and both the timing of sea ice advance and duration of ice cover (Ross et al., 2008). Superimposed on these long-term warming trends are decadal-scale climate oscillations, such as the El Niño Southern Oscillation (ENSO), that affect sea ice dynamics (e.g., Yuan, 2004; Stammerjohn et al., 2008b) and sea surface temperature (Renwick, 2002). ENSO has been linked to variability in Antarctic krill reproductive and recruitment success along the WAP (Quetin and Ross, 2003; Loeb, 2007; Loeb et al., 2009, Ross et al., 2014), and to the abundance of other species. There was no long-term directional trend in the abundance of salps in the Elephant Island region during the period 1993–2009, but rather a strong correlation with ENSO cycles (Loeb and Santora, 2012). In the same region and time period, abundance peaks in pteropods were also related to ENSO (Loeb and Santora, 2013).

The purpose of this study is to characterize interannual variability and long-term trends in major taxa of macrozooplankton (euphausiids, salps, pteropods, chaetognaths, polychaetes, and amphipods) along the WAP over two decades (1993–2013), primarily in the context of the north-south climate gradient, but also considering the coastal-shelf- offshore (slope) gradient. Our study, part of the PAL LTER program, adds up to an additional decade of macrozooplankton abundance data to previous analyses of this region of the WAP (Ross et al., 2008, 2014), compliments time-series analyses of the far northern Elephant Island region of the Peninsula as surveyed by the Antarctic Living Marine Resources (AMLR) program (Loeb et al., 2009; Loeb and Santora, 2012, 2013), and increases the breadth of the taxa considered. Further, we explore relationships between macrozooplankton abundance and a number of environmental parameters including: sea ice, atmospheric climate indices, sea surface temperature, and phytoplankton biomass (chl *a*) and productivity. Identification of long-term changes in zooplankton and the environmental factors affecting their abundance is key for predicting ecosystem change in this productive and sensitive polar ecosystem.

2. Materials and methods

2.1. Study area

The PAL LTER study region is located mid-way down the western side of the Antarctic Peninsula, and extends from Palmer Station on Anvers Island (64.77°S, 64.05°W) in the north to approximately 700 km south near Charcot Island (69.45°S, 75.15°W), and from coastal to slope waters approximately 200 km offshore (Ducklow et al., 2007, 2012a, 2012b) (Fig. 1). A grid of stations was sampled on PAL LTER annual research cruises during austral summer (approximately 01 January–10 February) each year aboard the MV *Polar Duke* (1993–1997) and ARSV *Laurence M. Gould* (1998-present). Grid lines perpendicular to the Peninsula are spaced 100 km apart, with stations along each line spaced 20 km apart (Waters and Smith, 1992) (Fig. 1). Prior to 2009 zooplankton were primarily collected from all stations on lines 600 to 200. While line 100 was sampled in 2007 and 2008, regular sampling of the far southern stations (lines 100, 000, and −100) began in 2009 in order to include an area with longer duration and greater extent of sea ice. From 2009, sampling intensity per line thus decreased due to time constraints. For most of our analyses, we either considered the entire grid ('Full Grid'), or divided the grid into latitudinal sub-regions based on hydrographic and sea-ice conditions (Martinson et al., 2008; Stammerjohn et al., 2008a) and a distinct change in penguin diet (W. Fraser pers. comm., Bernard et al., 2012) as follows: 'North' (lines 600, 500, and 400), 'South' (lines 300 and 200), and 'Far South' (100, 000, and −100) (Fig. 1). For multiple regression and other analyses as appropriate, we combined 'South' with 'Far South' data (referred to as 'South+' hereafter), and also considered the coastal-shelf-slope (on/off-shore) gradient. The latter is as defined by Martinson et al. (2008) (Fig. 1). As some samples were not collected at standard stations, for all sampling locations grid line was rounded to the nearest 100 km and grid station to the nearest 20 km to determine the appropriate regional designation.

2.2. Zooplankton collection and sample processing

Macrozooplankton were collected using a 2 m-square frame Metro net (700-μm mesh), towed obliquely to depths of ~120 m (Ross et al., 2008; Bernard et al., 2012). Net depth was determined real time with a depth sensor attached to the bottom of the conducting hydro wire and confirmed with a temperature-depth recorder. A General Oceanics flow meter positioned in the center of the net mouth was used to calculate volume filtered. The whole catch, or a subsample of the catch (depending on the density of macrozooplankton in the tow), was sorted by taxon on board, and the abundance and total biovolume (of fresh, unpreserved animals) of each species was determined. As in previous studies, we considered the five most dominant macrozooplankton species (which comprised on average 89% of total tow animal abundance and 97% of the total tow biovolume; see also Ross et al., 2008): the euphausiids *Euphausia superba*, *Thysanoessa macrura*, and *E. crystallorophias*; the tunicate (salp) *Salpa thompsoni*; and the thecosome (shelled) pteropod *Limacina helicina*. We also added several other common or conspicuous predatory taxa to our analysis, including the large chaetognaths *Pseudosagitta* spp.

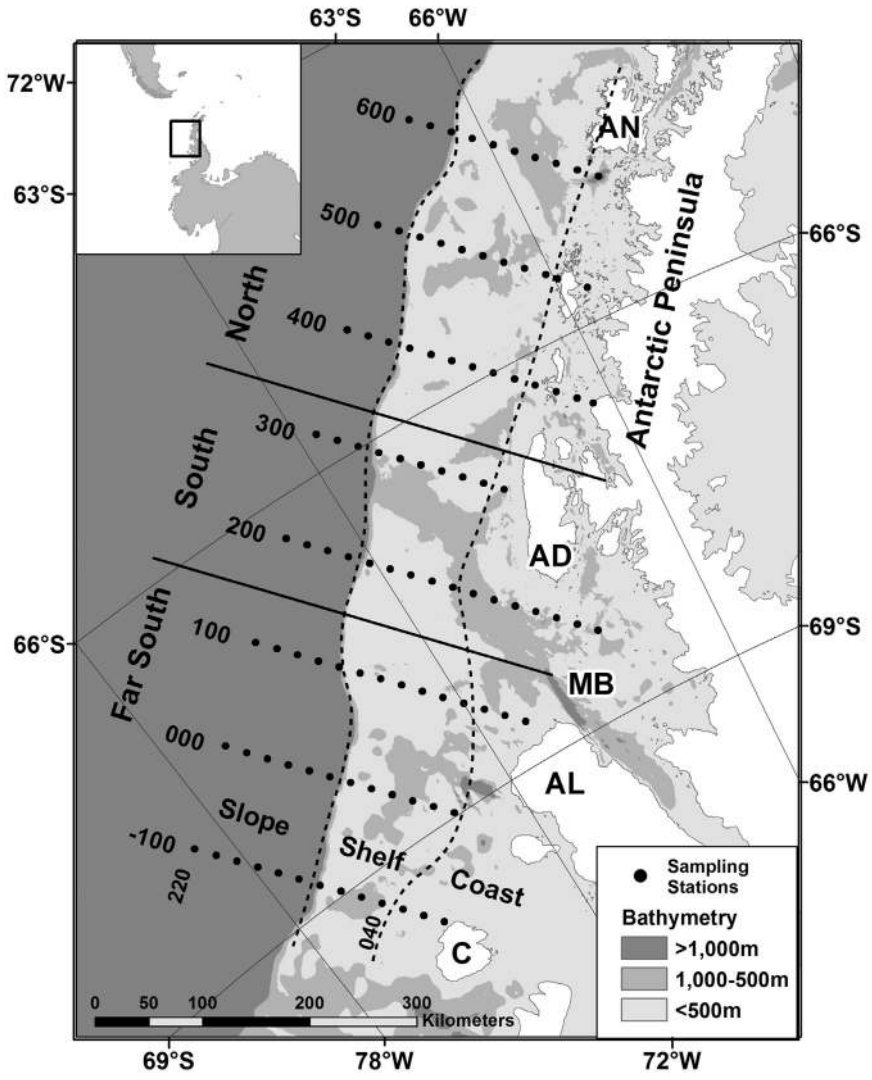

Fig. 1. Map of the Palmer Antarctica Long-Term Ecological Research (PAL-LTER) study region. Study region, highlighted by box, in relation to Antarctic continent (inset). AN: Anvers Island, AD: Adelaide Island, MB: Marguerite Bay, AL: Alexander Island, C: Charcot Island. LTER grid lines are numbered (from 600 to −100), and the far slope (220) and shelf (040) stations are indicated for reference (Waters and Smith, 1992). Palmer Station is located on Anvers Island. The Palmer Deep canyon is located just south of Anvers Island, and the Marguerite canyon is located just south of Adelaide Island. Solid lines separate the 'North', 'South', and 'Far South' sub-regions. Coastal, shelf, and slope regions are separated by dashed lines. All region divisions are based on hydrographic and sea-ice conditions (Martinson et al., 2008; Stammerjohn et al., 2008a). Shades of grey are used to illustrate the bathymetry, with light grey representing the continental shelf and dark grey the continental slope and abyssal plain. The continental shelf is roughly 200 km wide and averages 430 m in depth. Canyons cut the shelf and can approach depths of 1000 m. The light/dark gray interface indicates the shelf break at 1000 m, deepening to waters ~3000 m deep (Ducklow et al., 2012a).

(including *P. gazellae* and *P. maxima*), polychaete worms *Tomopteris* spp. (including *T. carpenteri*), the hyperiid amphipod *Themisto gaudichaudii*, and all 'other amphipod' taxa combined. The latter category was designated due to differences over time in identification of other amphipods to species level, and comprises mostly hyperiids (e.g., *Cyllopus lucasii*, *Hyperiella macronyx*, *Hyperoche medusarum*, *Primno macropa*, *Vibilia stebbingi*, and *Scina spp.*), and to a much lesser extent gammarids (e.g., *Eusiris* spp.). We present our analyses only as abundance data, as trends in biovolume closely mirrored that of abundance for all taxa. Note that large calanoid copepods were present in tows, but always constituted < 10% of total tow biomass, thus were not included in the scope of this study. Copepods were more completely sampled with a smaller mesh (335-μm) net towed to 300 m, and patterns in their abundance will be presented elsewhere (M. Gleiber and D. Steinberg, unpublished data).

We examined the effects of day vs. night sampling (i.e., potentially higher densities at night in surface waters due to diel vertical migration-DVM) on our results using an approach similar to Atkinson et al. (2008) and Ross et al. (2014). We determined sun elevation at the time and location of each tow (Meeus, 1998), with night defined as a sun elevation $\leq -0.833^{\circ}$. Night densities (n=170–187 tows, depending on taxon) were compared to day (n=848–951 tows) (Wilcoxon test, $p < 0.05$), and the mean night:day ratio (N:D) was determined for each taxon with significantly higher night density than day. These taxa included *S. thompsoni* (N:D=2.0), *T. gaudichaudii* (2.1), other amphipods (1.7), *L. helicina* (1.2), *T. macrura* (1.4), and *Tomopteris* spp. (1.7). As there were five-fold more day tows than night, we corrected (i.e., reduced) the night abundance values by dividing them by the N:D ratio to calculate a diel-corrected abundance. (We note that using corrected night tow data for our analyses in place of uncorrected data had only minor affects our results.)

2.3. Environmental parameters and climate indices

Several factors potentially affecting zooplankton abundance were considered, including: phytoplankton chlorophyll *a* (chl *a*) and

primary production (PP), sea-surface temperature (SST), sea-ice dynamics, and two climate indices. Chl *a* and PP were measured at each station from samples taken within the euphotic zone, as described in Vernet et al. (2008) and Ducklow et al. (2012a, 2012b). We integrated discrete measurements of chl *a* to 100 m, and PP to the deepest PP measurement (i.e., bottom of euphotic zone). SST was determined by the NOAA optimal interpolation (OI) sea surface temperature analysis (version OI.v2) using in situ and satellite SSTs, plus SSTs simulated by sea ice cover (for more detail see Reynolds et al., 2002). These data can be found at http://iridl.ldeo.columbia.edu/SOURCES/.NOAA/.NCEP/.EMC/.CMB/.GLOBAL/.Reyn_SmithOIv2/.monthly/.sst/. SST was averaged over the entire PAL grid and for the sub-regions (North, within 200 km south and west of Anvers Island; South, within 200 km south and west of Avian Island; Far South, within 200 km west of Alexander Island) (Fig. 1). Monthly data were used to obtain both annual and seasonal means (spring, Sept–Oct–Nov; summer, Dec–Jan–Feb; autumn, Mar–Apr–May; winter SST data were excluded in our analyses due to ice cover), and SST coincident with the time of zooplankton sampling (Jan).

Sea-ice parameters included extent, area, duration, number of ice days, date of advance, and date of retreat, and were derived from satellite imagery (Scanning Multichannel Microwave Radiometer and Special Sensor Microwave/Imager; SMMR-SSM/I) as described in Stammerjohn et al. (2008a). SMMR-SSM/I sea-ice concentration data are from the Earth Observing System Distributed Active Archive Center at the National Snow and Ice Data Center, University of Colorado (http://nsidc.org). 'Sea ice extent' is the total area within the sea ice edge, and 'sea-ice area' is the ocean area covered by sea ice, which excludes open areas inside the ice edge (both in km^2). Annual 'ice season duration' is the number of days between when sea ice first appears in the fall (year day of advance), and last appears in spring (year day of retreat), while actual 'sea ice days' are the number of days between the day of advance and retreat when ice concentration remained above 15% (Stammerjohn et al., 2008a). Sea-ice parameters were determined for the whole PAL LTER grid as well as our sub-regions (as described for SST above). All of the above data used in our analyses are available at: http://oceaninformatics.ucsd.edu/datazoo/data/pallter/datasets.

We also analyzed the relationship between macrozooplankton taxon abundance and climate indices known to influence the pelagic ecosystem of the Antarctic Peninsula region (Ross et al., 2008; Stammerjohn et al., 2008b; Loeb et al., 2009; Saba et al., 2014). These include the El Niño/Southern Oscillation (ENSO) indicator based on sea surface temperature–the Multivariate ENSO Index (MEI) (http://www.esrl.noaa.gov/psd/people/klaus.wolter/MEI/), as well as the Southern Annular Mode (SAM) (http://www.antarctica.ac.uk/met/gjma/sam.html) index based on sea level pressure. These climate indices are seasonally adjusted (e.g., Hurrell, 1995; Zhang et al., 1997). Similar to SST, we used both annual climate indices, and seasonal components of the indices (spring, Sept–Oct–Nov; summer, Dec–Jan–Feb; autumn, Mar–Apr–May; winter, Jun–Jul–Aug).

We tested relationships between taxon abundance and environmental forcing concurrent with the time of summer (Jan/Feb) sampling (0 lag; for chl *a*, PP, and SST) and with 1 and 2-year lags (i.e., prior 1 or 2 calendar years, or Jan/Feb periods, as appropriate; for all environmental parameters and climate indices). For example, a significant relationship between salp abundance in Jan. 2013 and a 1-year lag in ice retreat would indicate that the day of ice retreat in austral spring of 2012 affected salp abundance the following January. For SST and climate indices, the 'summer' season spans two calendar years (e.g., Dec 2012, Jan 2013, and Feb 2013). Thus, for the summer season, we use the calendar year of the end of the summer season to denote the lag (i.e., a significant relationship between salp abundance in Jan. 2013 and a 1-year lag in summer SST would indicate that variation in salp abundance was affected by summer SST in 2012 (mean of Dec 2011, Jan 2012, and Feb 2012).

2.4. Anomaly calculations

For each taxon and year in the time series, the abundance anomaly (A'_y) was calculated using the formula

$$A'_y = \log_{10}[\overline{A}_y/\overline{A}]$$

where $\overline{A}_y$ is the mean abundance for year *y*, and $\overline{A}$ is the mean of the yearly means (O'Brien et al., 2008). Anomalies were calculated for the entire grid, and also separately for different sub-regions. In the case of the latter, the relative magnitude of each annual anomaly should thus only be compared with others of the same taxon within the same sub-region, although it is appropriate to compare the direction of the anomaly (i.e., positive or negative) between taxa and sub-regions. The exception is for the analysis of variance (ANOVA), in which we tested differences between regions for each taxon (see below). Annual summer-time anomalies for chl *a*, PP, and SST, and annual anomalies for sea ice parameters were calculated in the same way as taxon abundance anomalies; climate indices are already in anomaly form. Climate indices do not have sub-regional anomalies.

2.5. Regional abundance

A three-way ANOVA, with data in annual anomaly form, was used to investigate broad-scale differences in regional abundance of each taxon, as well as gross differences in taxon abundance between the first (1993–2003) and second (2004–2013) halves of the time series (North/South+ x coast/shelf/slope x early/late time series). Multiple comparisons were adjusted with a Tukey correction.

2.6. Comparison with environmental parameters, climate indices, and among taxa

Stepwise multiple linear regression models, with data in annual anomaly form for the Full Grid, were used to assess the relative importance of the environmental and climate-forcing factors listed above in affecting abundance of the different taxa. Potential variables tested in the model thus included: chl *a*, PP, SST, the six ice variables, and two climate indices (both annual and seasonal components), with 0-, 1-, and 2-year lags. Only parameters that explained more than 10% of the variation (partial correlation) were included in the final model. The final model was assessed for outlying and influential observations, co-linearity, and normality of residuals. Positive autocorrelation was evaluated using the Durbin–Watson test (Neter et al., 1996). To further explore important parameters highlighted in above analyses, individual regressions were also calculated between time series (in annual anomaly form) of environmental parameters and climate indices and abundance of each taxon. We also tested for significant correlations between taxa. Significance for all statistical analyses was determined at $\alpha = 0.05$.

3. Results

3.1. Overall abundance by region

The most abundant taxa overall were the euphausiids (krill) *Thysanoessa macrura* and *Euphausia superba* (mean 203 and 111 ind. 1000 m^{-3}, respectively), followed by the pteropod *Limacina helicina*, salp *Salpa thompsoni*, and krill *Euphausia crystallorophias* (mean 65, 42, and 27 ind. 1000 m^{-3}, respectively) (Table 1, Full Grid). Large chaetognaths, tomopterid polychaetes, and amphipods were several orders of magnitude lower in abundance and each generally averaged < 10 ind. 1000 m^{-3} (Table 1). For most species maximum abundances were 2–3 orders of magnitude higher than the mean (Table 1). (Median abundance and interquartile range for each taxon can be found in Supplementary Table 1.) Two species showed significant

Table 1
Abundance of major taxa of macrozooplankton in the WAP. Mean abundance ± 1 standard deviation, SD, and maximum, Max (*note*: minimum abundance for all species was 0), for the entire time series (1993–2013). Shown is the Full Grid (all stations), the two latitudinal subregions (North and South+; each of which include Coast, Shelf, and Slope stations) and three offshore subregions (Coast, Shelf, and Slope; each of which include North and South+ stations). Full Grid, lines −100 to 600; North, lines 400–600; South+, lines −100 to 300 (entire southern region). Coast, Shelf, and Slope – see Fig. 1 for region locations (as well as grid lines mentioned above). Data include both day and night tows, with night data corrected (see Section 2). *Note*: values are calculated across the entire data set, i.e., annual means were not calculated first and then averaged for all years. The number of observations, *n* (in parentheses), is shown for each sub-region, as *n* varies slightly both within and between sub-regions – depending on the taxonomic resolution used over the time series for a given species, and due to unequal number of sampling stations between each sub-region, respectively. See Supplementary Table 1 for median abundance data.

Taxon	Abundance by region (individuals 1000 m^{-3})											
	Full Grid		North		South+		Coast		Shelf		Slope	
	Mean SD	Max	Mean SD	Max	Mean SD	Max	Mean SD	Max	Mean SD	Max	Mean SD	Max
Krill												
Euphausia superba	111 ± 580	10592	96 ± 473	9901	131 ± 691	10592	182 ± 776	10592	102 ± 539	9901	20 ± 52	384
Euphausia crystallorophias	27 ± 143	2549	21 ± 95	1068	34 ± 185	2549	68 ± 239	2549	9.7 ± 47	712	0.2 ± 1.3	17
Thysanoessa macrura	203 ± 558	8446	244 ± 688	8446	153 ± 327	3765	106 ± 258	2811	248 ± 716	8914	255 ± 452	3765
Salp												
Salpa thompsoni	42 ± 364	10521	35 ± 148	2291	51 ± 520	10521	6.9 ± 27	276	13 ± 48	639	173 ± 806	10521
Pteropod												
Limacina helicina	65 ± 168	4038	57 ± 103	837	74 ± 225	4038	41 ± 131	1410	65 ± 197	4038	104 ± 135	1011
Chaetognaths												
Pseudosagitta spp.	1.2 ± 2.2	27	1.3 ± 2.5	27	1.1 ± 1.7	10	0.9 ± 1.4	10	1.7 ± 2.6	27	0.6 ± 1.7	19
Polychaetes												
Tomopteris spp.	0.4 ± 1.2	19	0.4 ± 1.0	10	0.5 ± 1.4	19	0.1 ± 0.4	6.2	0.2 ± 0.6	5.9	1.4 ± 2.2	19
Amphipods												
Themisto gaudichaudii	6.8 ± 22	310	6.2 ± 21	310	7.5 ± 23	307	1.3 ± 3.3	28	6.9 ± 19	268	16 ± 38	310
Other amphipods	3.0 ± 6.5	92	2.7 ± 6.2	87	3.4 ± 6.8	92	2.6 ± 4.6	50	2.4 ± 5.3	87	5 ± 10	92
***n* for each region**	(1021–1141)		(557–632)		(464–509)		(328–370)		(484–547)		(205–226)	

latitudinal differences. *T. macrura* was overall more abundant in the North vs. the South+ ($p < 0.01$, ANOVA; Table 1), and *L. helicina* was significantly more abundant in the North and South+ slope regions, and least abundant in the North and South+ coast regions ($p = 0.03$, ANOVA, interaction between North/South+ **x** across-shore gradient, North coast < North shelf, North slope, and South+ slope; North slope > South+ coast and South+ shelf; Table 1).

For the on/offshore gradient, *E. superba* was significantly more abundant on the coast and shelf than the slope ($p < 0.001$, ANOVA; Table 1), and *E. crystallorophias* significantly increased in abundance closer to the coast (coast > shelf > slope, $p < 0.0001$, ANOVA; Table 1). Moving further offshore, *T. macrura* was significantly more abundant over the shelf than the coast ($p = 0.03$, ANOVA; Table 1), and large chaetognaths (*Pseudosagitta* spp.) were highest in abundance over the shelf (shelf > coast > slope, $p < 0.0001$, ANOVA; Table 1). At the slope end of the on/offshore gradient were the salps, amphipods (*Themisto gaudichaudii* and all other amphipods), and tomopterid polychaetes, which were all more abundant on the slope than the shelf and coast ($p = < 0.0001$, < 0.0001, < 0.0001, and 0.04, respectively, ANOVA; Table 1).

3.2. Long-term changes in north vs. south by taxon

There was no overall long-term change in Antarctic krill, *E. superba*, abundance over the 20-year period (Fig. 2a). However, anomalies of *E. superba* abundance showed a clear 4–6 year cycle, with abundance peaks–usually 2 sequential years of increasing positive anomalies–followed by 3–4 sequential years of negative anomalies, especially in the North (Fig. 2a). Spectral analysis of *E. superba* abundance anomalies for the Full Grid confirmed a significant 5-year periodicity (Fig. 3). Large, positive anomalies in *E. superba* in the North, South, and Far South occurred in 2012 and 2013. There was no long-term trend in ice krill, *E. crystallorophias*, abundance in the North, but a significant increase in abundance occurred in the South (Fig. 2b). In addition, *E. crystallorophias* anomalies overall shifted to positive in the latter half of the time series (post-2003) ($p = 0.01$, ANOVA). Abundance of *T. macrura* increased over the long term, also with a shift from negative to increasingly positive anomalies post-2003, in both the North and South (Fig. 2c; $p < 0.0001$, ANOVA).

Both salp (*S. thompsoni*) and pteropod (*L. helicina*) abundance in the North alternated between positive and negative anomalies that typically persisted for 2-4 (salps) or 2-6 (pteropods) consecutive years (Fig. 4a and b), but spectral analysis indicated no significant periodicity of these cycles for either species ($p > 0.05$). In the South, there is an indication of an increase over the long term for both species, with more and larger negative anomalies characterizing the earlier half of the time series, and increasing positive anomalies later, until 2012 and 2013 (high *E. superba* abundance years) when both salp and pteropod abundance was low (Fig. 4a and b).

The gelatinous carnivores, *Pseudosagitta* spp. chaetognaths and *Tomopteris* spp. polychaetes, generally increased in abundance, although patterns varied between the North and South regions. For *Pseudosagitta* spp., while there were a few single high positive years during the first part of the time series in the North, after 2006 there are more consecutive positive anomalies (Fig. 5a). In the South, there is more of an alternating pattern in abundance, but in the Far South anomalies trend from negative to positive suggesting an increase (Fig. 5a). *Tomopteris* spp. abundance significantly increased over the time series, with a switch from negative to positive anomalies in 2007 in the North, and in 2006 in the South (Fig. 5b). In the Far South, anomalies also trend from negative to positive (Fig. 5b). The ANOVA for both *Pseudosagitta* spp. and *Tomopteris* spp. also indicated a significant increase in the latter half of the time series ($p = 0.03$ and 0.02, respectively).

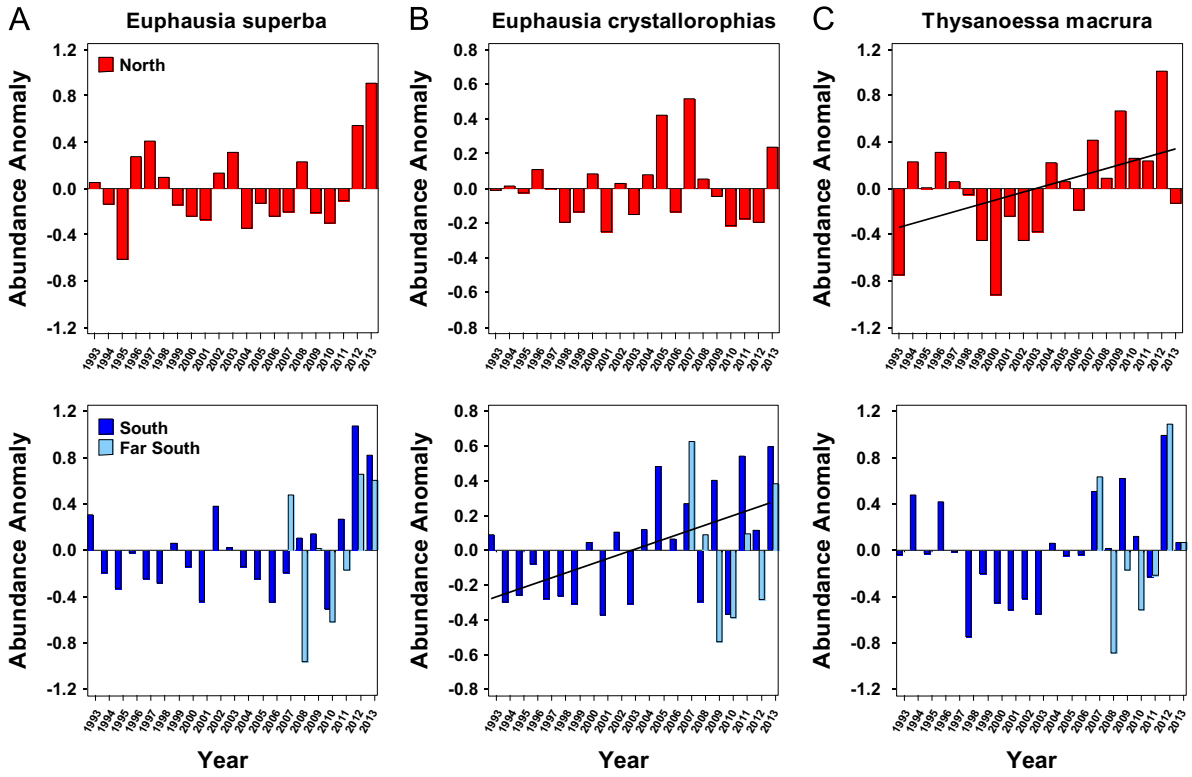

Fig. 2. Annual abundance anomalies of euphausiid species. (A) Antarctic krill, *Euphausia superba*, (B) Ice krill, *Euphausia crystallorophias*, and (C) *Thysanoessa macrura*. Upper plots are the 'North' sub-region (lines 600, 500, and 400), and lower plots 'South' (300 and 200 lines) and 'Far South' (100, 000, and −100 lines) sub-regions. Anomalies were calculated separately for each species and sub-region (thus relative height or depth of bars should only be compared with others of the same species and sub-region). Regression lines indicate significant linear relationships (*E. crystallorophias*, South, $p=0.01$, $r^2=0.29$; *T. macrura*, North, $p=0.03$, $r^2=0.22$).

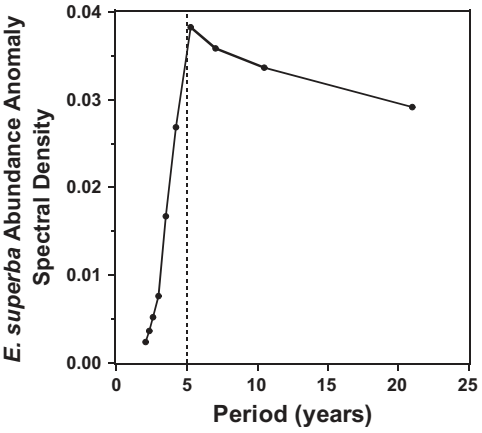

Fig. 3. Spectral analysis of *Euphausia superba* abundance anomalies for the full sampling grid. Analysis indicates a significant 5-year periodicity ($p=0.02$, Bartlett's Kolmogorov–Smirnov statistic, Fuller, 1996); dashed line at 5 years is for reference.

There was no long-term pattern in abundance of the common amphipod *T. gaudichaudii*, which over time switched between negative and positive anomalies at non-regular intervals (Fig. 6a). The abundance of all other amphipods combined increased significantly in the South (Fig. 6b), and overall there were significantly more 'other' amphipods in the latter half of the time series regardless of region ($p=0.02$, ANOVA).

3.3. Antarctic krill vs. salps, and other pairwise taxa comparisons

As *E. superba* and *S. thompsoni* have been hypothesized to occupy different ecological niches (Pakhomov et al., 2002), we conducted a pairwise comparison of their abundances in each tow across the entire sampling grid and time series (Fig. 7). Although the two species regularly co-occur, at high abundances of either species there was a clear separation in their occurrence in time and space. Instances of high *E. superba* abundance corresponded to low *S. thompsoni* abundance, and visa versa; high abundance of *E. superba* occurred in coastal and shelf stations, while that of salps occurred over the slope (Fig. 7). At low to intermediate abundance, the two species were more likely to co-occur, but there was still some spatial separation (Fig. 7, inset). Contingency table analysis of *E. superba* and *S. thompsoni* presence/absence confirmed that the occurrence of the two species were not independent, and were negatively associated (continuity adjusted chi-square, $p<0.01$, phi coef.$=-0.08$, $n=1135$). This result is mainly due to the slope stations where salps are predominant ($p=0.02$, phi coef.$=-0.17$, $n=224$; coast and shelf were not significant).

We also performed correlation analyses on annual anomalies of *E. superba* vs. *S. thompsoni* and all other pairwise combinations of major taxa for the Full, North, and South+ (entire south) grid. Although at this resolution there was no significant negative correlation between *E. superba* vs. *S. thompsoni*, there were several statistically significant relationships between other pairs of taxa (Table 2). In particular, *E. superba* was positively correlated with 'other' amphipods and with *E. crystallorophias*, especially in the South+. In the North, both *Pseudosagitta spp.* and *T. macrura* were positively correlated with *Tomopteris spp.*, and 'other' amphipods were positively correlated with *L. helicina* (Table 2).

3.4. Relationship with environmental parameters and climate indices

Time series of some of the most important environmental parameters and climate indices explaining variability in WAP zooplankton abundance are shown in Figs. 8 and 9. The sign and magnitude of the

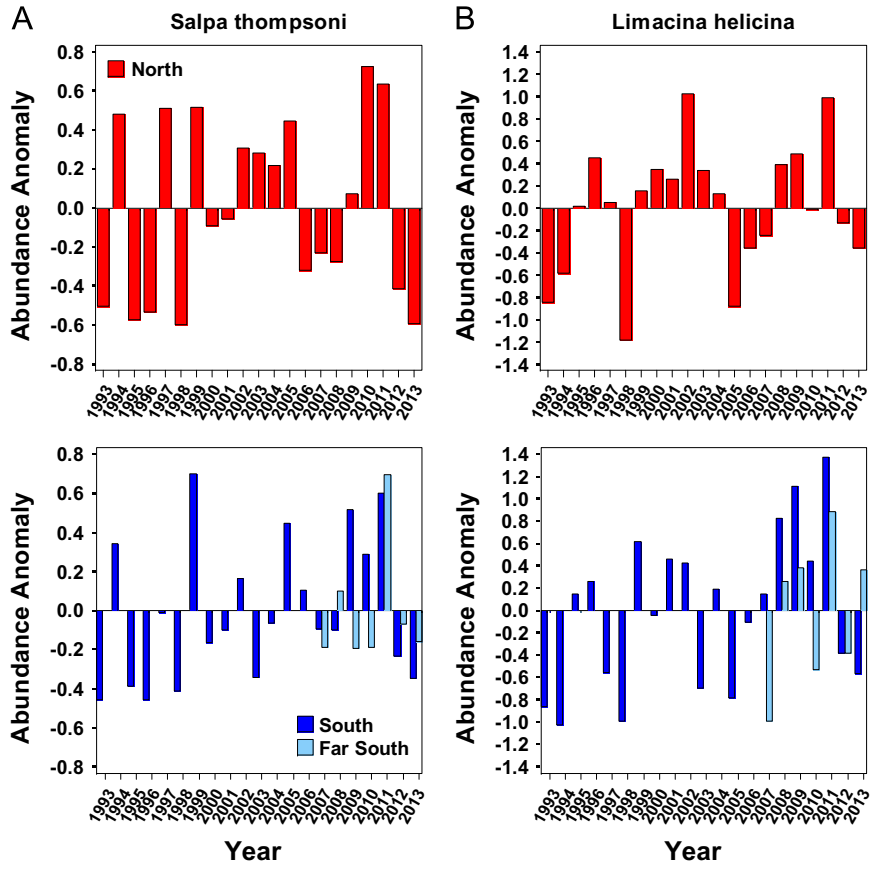

Fig. 4. Annual abundance anomalies of salps and pteropods. (A) salp, *Salpa thompsoni*, (B) thecosome pteropod, *Limacina helicina*. Upper plots are the 'North' sub-region (lines 600, 500, and 400), and lower plots 'South' (300 and 200 lines) and 'Far South' (100, 000, and −100 lines) sub-regions. Anomalies were calculated separately for each taxon and sub-region (thus relative height or depth of bars should only be compared with others of the same species and sub-region).

annual MEI (Fig. 8a) is closely tracked by all four seasonal MEI indices (Fig. 8b), and shows the strong 1997/98 El Niño (positive index) followed by a La Niña period (negative). Beginning in 2002, MEI is positive for 5 years before changing sign again. The annual SAM index indicates a large positive anomaly also occurred in 1998 (Fig. 8c), and the seasonal indices of SAM are variable and do not always track the annual index (Fig. 8d). Ice area (Fig. 9a) and ice days (Fig. 9b) anomalies track each other closely in sign and magnitude. Ice area and days decrease significantly in all areas over time for all regions ($p<0.05$) and anomalies switch from largely positive to negative over the course of the time series. However, there are embedded extended periods of positive ice anomalies (2002–2005), that correspond with negative spring SST anomalies, and a very low negative sea ice anomaly and high positive spring SST in 2008 (Fig. 9a–c). January SST increased, although not significantly, over the time series (Fig. 9d) and anomalies were positively correlated with prior year spring SST (Full Grid, $p=0.02$, $r^2=0.26$; South+, $p=0.03$, $r^2=0.23$). PP increased significantly over the time series (Full Grid, $p=0.03$, $r^2=0.26$; South+, $p<0.01$, $r^2=0.37$), with peaks in positive anomalies occurring every 4–6 years (Fig. 9e). Peaks in chl *a* coincided with high PP years, but there was no long-term increase in chl *a* ($p>0.05$) (Fig. 9f).

For the two most abundant euphausiid species, *E. superba* and *T. macrura*, PP with a 2-year lag explained the greatest proportion of the variation in abundance in our stepwise multiple regression analyses (partial R^2 of 0.71 and 0.38, respectively; Table 3). This relationship was significant and positive for *E. superba* regardless of the region (Full, North, South+), and for *T. macrura* for Full Grid and South+ (Fig. 10a and b). SST (autumn and Jan., 2-year lag) also was a significant predictor of *T. macrura* abundance. The most important explanatory parameter for *E. crystallorophias* was SAM (summer, 1-year lag), with MEI also significant (winter, 1-year lag) (partial $R^2=0.31$ and 0.19, respectively; Table 3); both were negatively correlated with abundance anomalies (Table 3). *E. crystallorophias* was also more abundant following higher ice conditions, especially in the Far South, as indicated by their significant positive relationship with ice days, retreat, extent, area, and duration (1–2 year lag; $p=0.02$–0.03, $r^2=0.65$–0.70), and negative relationship with date of sea ice advance (1-year lag, $p<0.01$, $r^2=0.88$).

Climate and SST parameters accounted for most of the variation in salp (*S. thompsoni*) and pteropod (*L. helicina*) abundance. For *S. thompsoni*, SAM (winter) and MEI (winter) (partial $R^2=0.25$ and 0.14, respectively), and for *L. helicina* MEI (winter) and spring SST (partial $R^2=0.55$ and 0.16, respectively), the year prior, were most important (Table 3). In further exploration, we found that *S. thompsoni* was most highly positively correlated with SAM (winter) the year prior in the South+ (Fig. 11a). In every region, *L. helicina* abundance was significantly negatively correlated with the year prior MEI (annual, and all seasonal components except autumn) (e.g., Fig. 11b), and warmer spring SST led to higher summer *L. helicina* abundance (Fig. 11c). It was also evident that both species are adverse to high ice conditions. For *S. thompsoni*, the most significant negative relationships between ice (area and days) and abundance occurred in the South (Fig. 11d), and these negative correlations were even stronger for *L. helicina* in the South (Fig. 11e).

For *Pseudosagitta* spp. chaetognaths, SAM (annual, 2-year lag) and PP (no lag) explained the greatest proportion of the variation in the model (partial $R^2=0.29$ and 0.24, respectively), with SAM (winter) and sea ice days also significant. For *Tomopteris spp.* polychaetes, SST (autumn, 2-year lag) was the strongest parameter explaining

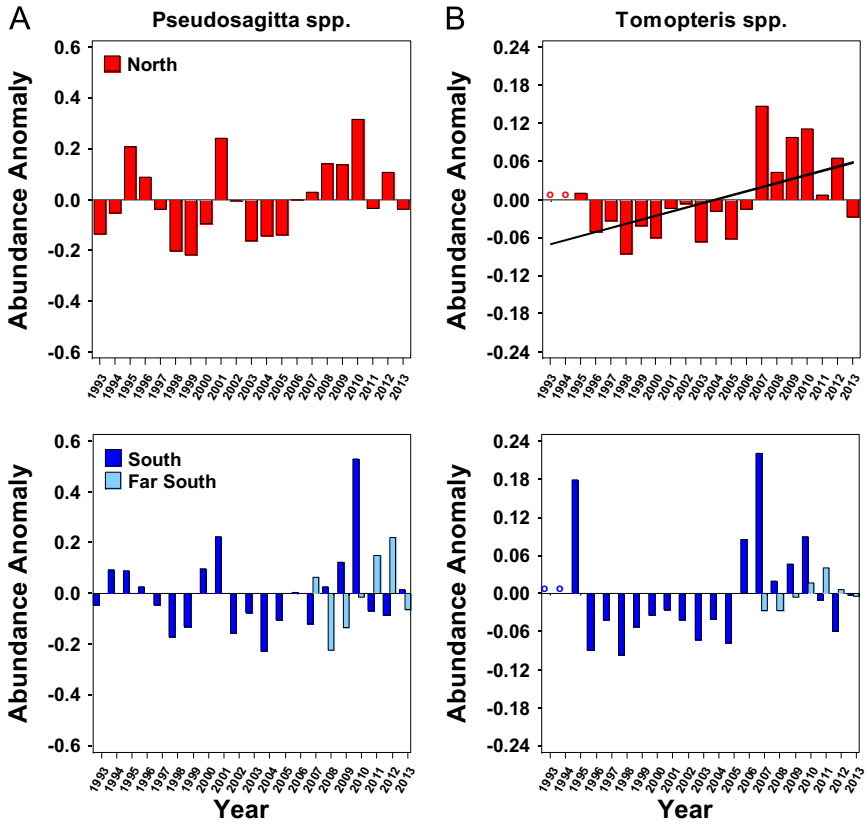

Fig. 5. Annual abundance anomalies of gelatinous carnivores. (A) chaetognaths, *Pseudosagitta* spp., and (B) polychaete worms, *Tomopteris spp*. Upper plots are the 'North' sub-region (lines 600, 500, and 400), and lower plots 'South' (300 and 200 lines) and 'Far South' (100, 000, and −100 lines) sub-regions. Anomalies were calculated separately for each taxon and sub-region (thus relative height or depth of bars should only be compared with others of the same species and sub-region). Open circles indicate no data for taxon that year. Regression line indicates a significant linear relationship (*Tomopteris spp*., North, $p=0.01$, $r^2=0.30$).

variability in abundance (partial $R^2=0.42$) with SAM (autumn, 1-year lag) and chl *a* (no lag) also important (0.13, and 0.18, respectively) (Table 3). In exploring these relationships further by region, we found that *Pseudosagitta* abundance was significantly positively correlated with SAM regardless of latitudinal region (Fig. 12a) for SAM annual and spring indices (2-year lag) ($p=0.001$–0.05, $r^2=0.19$–0.44), but most strongly in the South+ ($r^2=0.44$, spring, 2-year lag). A strong relationship between sea ice and both *Pseudosagitta* and *Tomopteris* abundance was also apparent. For example, we found significant negative correlations between nearly all ice parameters tested and *Pseudosagitta* abundance, again particularly in the South and with a 2-year lag (e.g., Fig. 12b).

The MEI (spring, year prior) and SAM (autumn, year prior) explained the most variability in abundance of other amphipods (partial $R^2=0.24$ and 0.26, respectively), with SAM (summer, 2-year lag) also significant; all were negatively correlated with other amphipod abundance (Table 3).

4. Discussion

4.1. Euphausiid patterns of abundance and links with primary production, ice, and climate

We did not find a long-term decrease in Antarctic krill, *E. superba*, unlike the decrease reported for the SW Atlantic sector of the Southern Ocean (Atkinson et al., 2004) and for the CCAMLR study region in the far northern WAP (Loeb et al., 1997). These long-term decreases in *E. superba* north of the PAL LTER survey grid have been attributed to trends in regional warming and decreasing ice cover. On a finer spatial scale in the 1993–2008 period, Ross et al. (2014) documented a ~200 km shift southward of highest abundances in Antarctic krill, but also no long-term trend.

The repeating pattern of a ~5 year cycle in abundance peaks, as indicated by high positive anomalies, corresponds well with a reported average ~5 year repeating cycle of strong krill recruitment events (i.e., winter survival of larvae and juveniles), as indicated by the frequency of occurrence of the 16 to 25 mm krill size class (the +1 age class) in penguin stomachs near Palmer Station (Fraser and Hofmann, 2003, years 1973–1997; Saba et al., 2014, years 1988–2012) and krill length-density distributions derived from net tows along the WAP (Quetin and Ross, 2003; Ross et al., 2014, years 1993–2008). For the latter, 2 good recruitment years (high numbers of 1-year-olds, AC1s) were followed by 3 or 4 with few AC1s (Quetin and Ross, 2003; Ross et al., 2014). This corresponds well with the repeating cycle we found of two sequential high abundance years with the anomaly in the 2nd year greater than that of the 1st year, followed by 3 or 4 years with decreasing and usually negative anomalies. The higher positive anomaly in the 2nd year of the cycle results from the accumulation of krill from two good recruitment years, i.e., when both of the sequential year classes (AC1s and AC2s) are abundant.

These strong recruitment years coincide with several environmental factors: a 4–5 year cycle of high winter sea ice extent (Fraser and Hofmann, 2003), neutral or moderate periods of ENSO creating good ice conditions for reproduction in summer and larval survival in winter (Quetin and Ross, 2003; Ross et al., 2014), and positive anomalies in chl *a* the preceding year, resulting from physical forcing and a negative phase of SAM (Saba et al., 2014). We found *E. superba* abundance peaks followed large peaks in PP that occurred 2 years prior (see below). Indeed, the 5–6 year *E. superba* life span has been suggested as an evolved strategy that

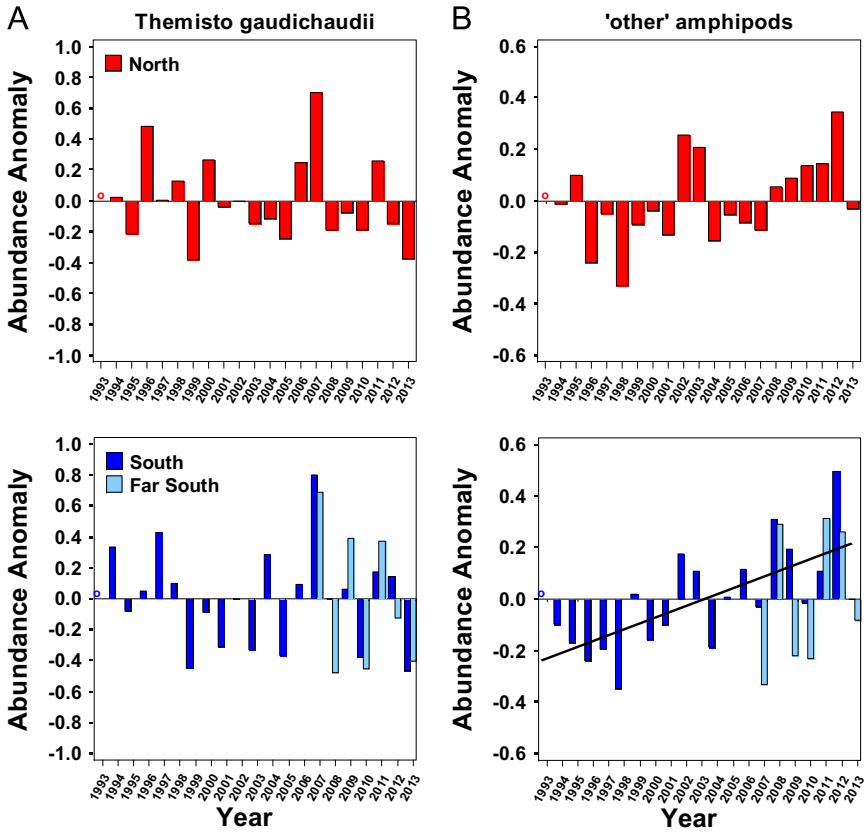

Fig. 6. Annual abundance anomalies of amphipods. (A) hyperiid amphipod, *Themisto gaudichaudii*, and (B) all other amphipods combined. Upper plots are the 'North' sub-region (lines 600, 500, and 400), and lower plots 'South' (300 and 200 lines) and 'Far South' (100, 000, and −100 lines) sub-regions. Anomalies were calculated separately for each taxon and sub-region (thus relative height or depth of bars should only be compared with others of the same species and sub-region). Open circles indicate no data for taxon that year. Regression line indicates a significant linear relationship (other amphipods, South, $p < 0.01$, $r^2 = 0.45$).

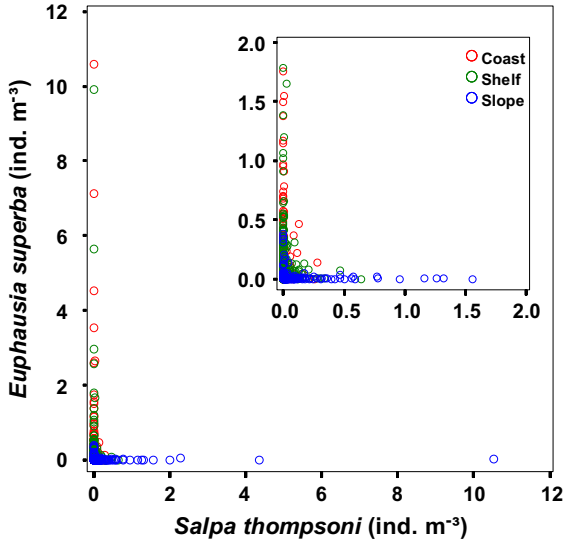

Fig. 7. Pairwise comparison of abundance of *Euphausia superba* and *Salpa thompsoni*. Data shown are abundance in each tow across the entire sampling grid and time series for tows containing one or both species. Colors indicate where tow was taken along the WAP coastal-shelf-slope gradient. Inset: Scale expanded to show further details of pattern at lower abundances.

Table 2
Pair-wise comparisons of major macrozooplankton taxa in the WAP. Correlation analysis was performed on annual anomalies for the entire time series (1993–2013) for the different grid regions: Full, lines −100 to 600; North, lines 400–600; and South+, lines −100 to 300 (entire southern region); see Fig. 1 for location of grid lines and region locations. 'Other amphipods' are all amphipods except *Themisto gaudichaudii*. All possible pair-wise combinations of taxa for each grid sector were tested; only statistically significant correlations ($p \leq 0.05$) are shown.

Taxa comparison	Grid region	r^2	*p*-Value	Slope	*n*
Euphausia superba vs. other amphipods	Full	0.214	0.040	1.002	20
Euphausia superba vs. other amphipods	South+	0.308	0.011	1.183	20
Euphausia superba vs. *E. crystallorophias*	South+	0.275	0.015	0.636	21
Pseudosagitta spp. vs. *Tomopteris spp.*	Full	0.213	0.047	1.005	19
Pseudosagitta spp. vs. *Tomopteris spp.*	North	0.416	0.003	1.530	19
Thysanoessa macrura vs. *Tomopteris spp.*	North	0.385	0.005	4.176	19
other amphipods vs. *Limacina helicina*	North	0.214	0.040	0.140	20

minimizes mismatches between krill and their food caused by environmental variability (Fraser and Hofmann, 2003) and allows the population to thrive with only 2 good recruitment years out of 5 (Siegel, 2005). How this cyclic pattern may change with respect to shifting climate patterns and multiple environmental stressors on krill– such as ocean warming, changing circulation patterns, ocean acidification, and changing UV radiation (Flores et al., 2012) remains to be seen. Recent experiments exposing *E. superba* to enhanced carbon dioxide caused shifts in physiology and metabolism consistent with increased physiological costs, which could negatively impact krill growth and reproduction (Saba et al., 2012); warming could be expected to do the same, as growth

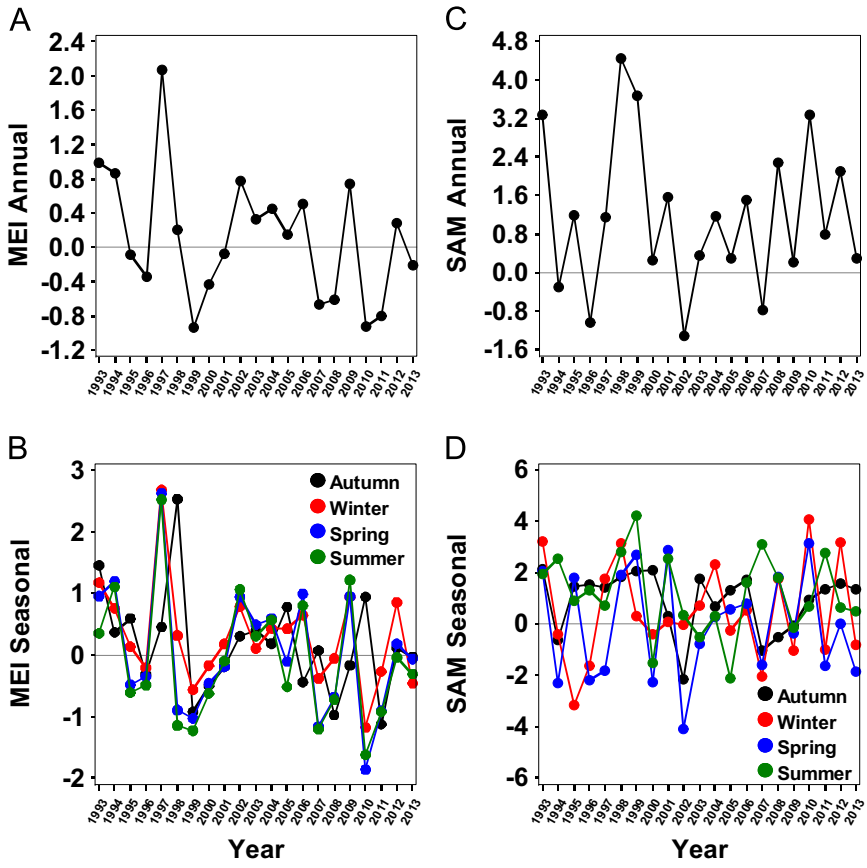

Fig. 8. Time series of climate indices. (A) Multivariate ENSO index (MEI) annual, (B) MEI seasonal, (C) Southern Annular Mode (SAM) annual index, and (D) SAM seasonal indices.

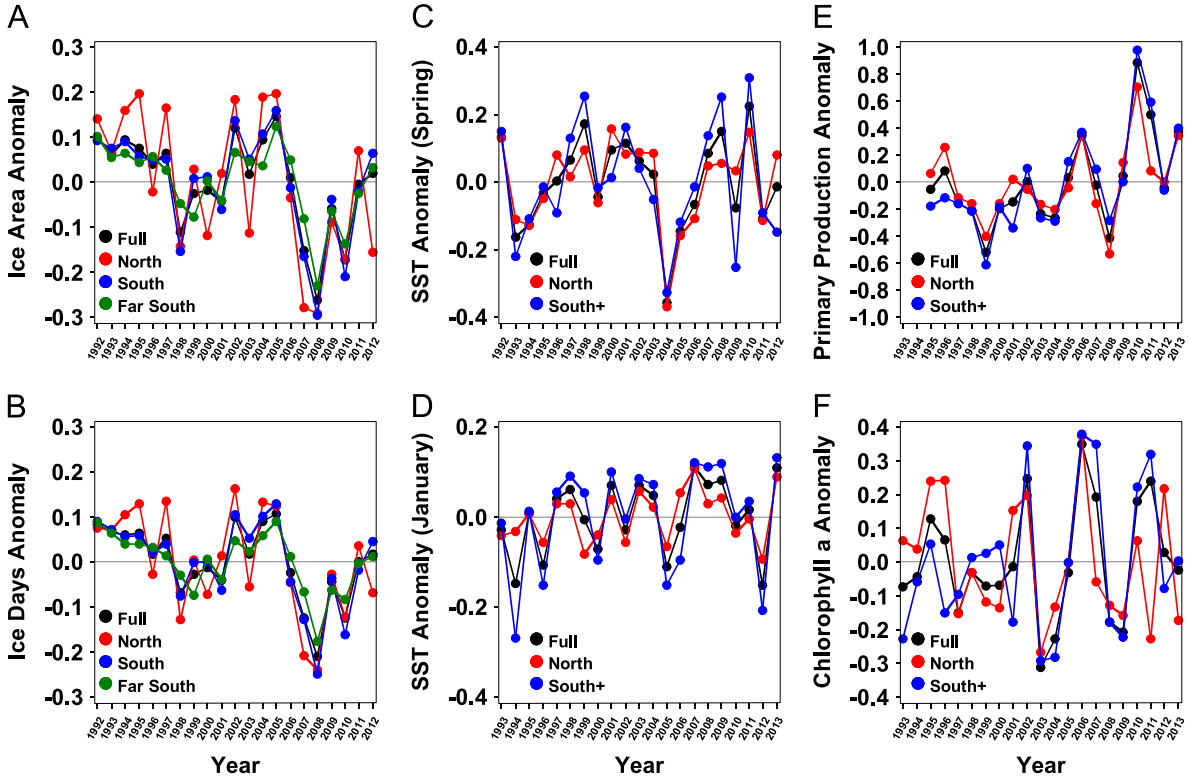

Fig. 9. Time series of WAP sea ice, SST, primary production, and chlorophyll *a* anomalies. Data plotted are annual anomalies for different grid regions as indicated ('South+' is 'South' and 'Far South' regions combined; lines 300 to −100). (A) Ice area, (B) Ice days, (C) Spring SST, (D) January SST, (E) Primary production, and (F) Chlorophyll *a*. Note different *x*-axis scales.

Table 3
Results of stepwise multiple regression analyses addressing the effect of environmental parameters and climate on WAP zooplankton abundance. Explanatory variables and statistical scores obtained from the best model among stepwise multiple regression analyses are shown. Climate indices: SAM, Southern Annular Mode; MEI, Multivariate El Niño Southern Oscillation index. Test statistics include R^2, p-values, and sample size (n) for the overall model, the coefficient (slope) for the regression equation, the standard error (SE) associated with the model coefficient, the 2 tailed p-value (p) used in testing the null hypothesis for each significant model variable, and the partial R^2. *Themisto gaudichaudii* model was unstable due to co-linearity (Belsley et al., 1980) and is not presented.

Variable	*n*	Coefficient	SE	*P*	*Partial R²*
Euphausia superba (R^2=0.71, p= < 0.001)	17				
Primary production (2-year lag)		0.913	0.151	< 0.001	0.710
Euphausia crystallorophias (R^2=0.50, p= < 0.01)	20				
SAM (summer, 1-year lag)		−0.081	0.023	0.002	0.311
MEI (winter, 1-year lag)		−0.117	0.047	0.023	0.185
Thysanoessa macrura (R^2=0.73, p= < 0.001)	17				
Primary production (2-year lag)		0.723	0.178	0.001	0.376
Sea surface temperature (autumn, 2-year lag)		−7.750	1.880	0.001	0.237
Sea surface temperature (Jan., 2-year lag)		2.525	1.062	0.034	0.117
Salpa thompsoni (R^2=0.39, p=0.01)	21				
SAM (winter, 1-year lag)		0.099	0.034	0.010	0.252
MEI (winter, 1-year lag)		−0.175	0.086	0.056	0.141
Limacina helicina (R^2=0.71, p= < 0.001)	21				
MEI (winter, 1-year lag)		−0.461	0.092	0.0001	0.546
Sea surface temperature (spring, 1-year lag)		1.701	0.535	0.0052	0.164
Pseudosagitta spp. (R^2=0.80, p= < 0.001)	19				
SAM (annual, 2-year lag)		0.036	0.010	0.004	0.292
Primary production (0-year lag)		0.208	0.048	0.001	0.235
SAM (winter, 1-year lag)		−0.033	0.009	0.003	0.136
Sea ice days (1-year lag)		−0.606	0.198	0.009	0.135
Tomopteris sp. (R^2=0.73, p= < 0.001)	19				
Sea surface temperature (autumn, 2-year lag)		−1.317	0.248	< 0.001	0.419
SAM (autumn, 1-year lag)		−0.025	0.007	0.004	0.134
Chlorophyll *a* (0-year lag)		0.146	0.047	0.007	0.176
Other amphipods* (R^2=0.65, p= < 0.001)	20				
MEI (annual, 1-year lag)		−0.130	0.033	0.001	0.242
SAM (autumn, 1-year lag)		−0.082	0.021	0.001	0.257
SAM (summer, 1-year lag)		−0.041	0.016	0.021	0.146

* Durbin–Watson test for positive autocorrelation significant for this taxon (p=0.03).

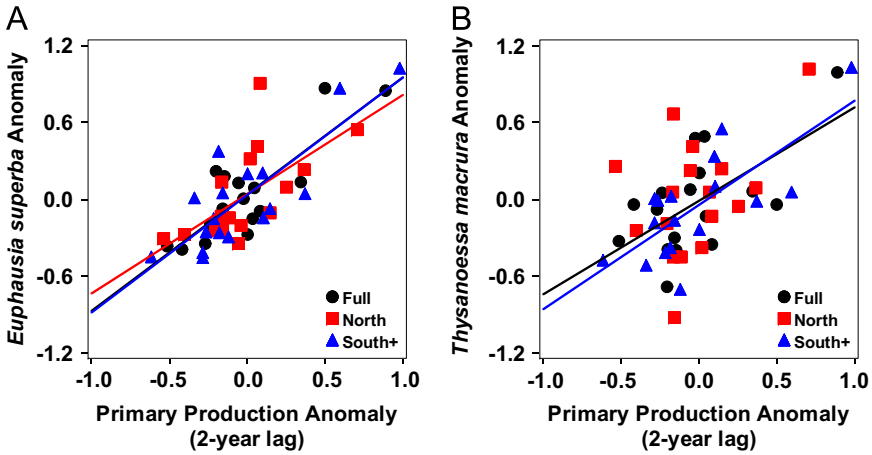

Fig. 10. Increase in the two most abundant krill species with primary production. (A) *Euphausia superba*, and (B) *Thysanoessa macrura*. Data plotted are annual anomalies for each year of the time series (1993–2013) for different grid regions as indicated ('South+' is 'South' and 'Far South' regions combined; lines 300 to −100). Primary production (PP) is lagged 2-years behind krill abundance (e.g., 2013 krill annual anomaly is plotted against 2011 PP annual anomaly). Regression lines for significant linear relationships are shown. *Euphausia superba*: Full Grid, $p < 0.0001$, r^2=0.71; North, $p < 0.01$, r^2=0.40; South+, $p < 0.0001$, r^2=0.69. *Thysanoessa macrura*: (full, $p < 0.01$, r^2=0.38; South+, p=0.001, r^2=0.55).

does not occur above a temperature threshold (Atkinson et al., 2006).

Abundance of *T. macrura* significantly increased in the North over the course of the time series, likely directly or indirectly a consequence of increasing PP (see below). *T. macrura* is known to be a widely distributed, omnivorous species that unlike *E. superba*, rarely forms schools and is not thought to closely associate with sea ice (Daly and Macaulay, 1988; Flores et al., 2012; Haraldsson and Siegel, 2014). Seasonal and life history studies of *T. macrura* indicate they undergo seasonal vertical migration and may live up to 5 years (Haraldsson and Siegel, 2014). The one prior report on long-term, interannual changes in *T. macrura* abundance indicates no long-term trend for the WAP over the period 1993–2004 (Ross et al., 2008). However a change in the sign of anomalies from positive to negative occurred between

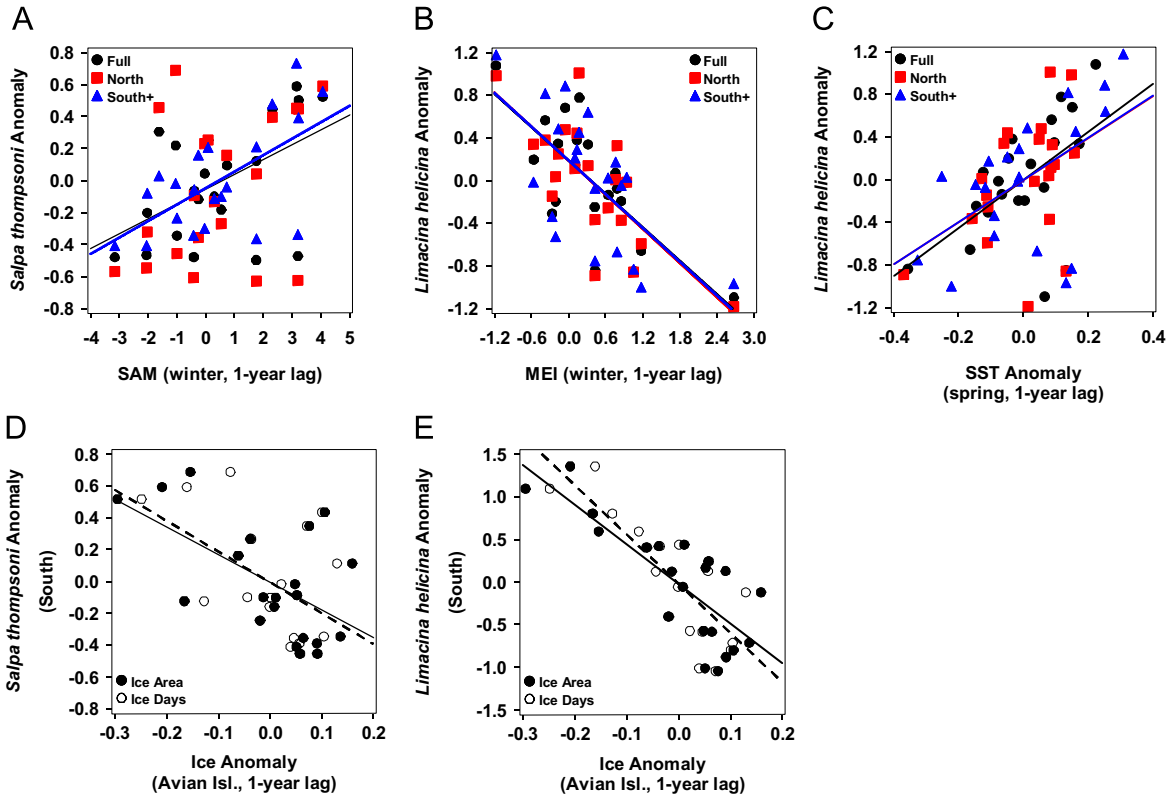

Fig. 11. Effect of sub-decadal climate oscillations, sea surface temperature, and sea ice on abundance of salps and pteropods. (A) Southern Annular Mode (SAM) winter index (year prior) vs. *Salpa thompsonii*, (B) Multivariate El Niño Southern Oscillation Index (MEI) winter (year prior) vs. *Limacina helicina*, (C) Sea surface temperature (SST) spring anomaly (year prior) vs. *Limacina helicina*, (D) Ice area and Ice days (Avian Island, year prior) vs. *Salpa thompsonii* for the South region, (E) Ice area and Ice days (Avian Island, year prior) vs. *Limacina helicina* for the South region. Data plotted are annual anomalies for each year of the time series (1993–2013) for indicated regions ('South+' is 'South' and 'Far South' regions combined; lines 300 to −100). In (D) and (E), Avian Island is the 'South' ice sub-region, within 200 km south and west of Avian Island (See Methods); solid and dashed regression lines correspond to ice area and days, respectively. Regression lines for significant linear relationships are shown; statistics are as follows ($n=21$ for each, NS=not significant): (A) full, $p=0.02$, $r^2=0.25$; North, NS; South+, $p<0.01$, $r^2=0.37$, (B) full, $p<0.001$, $r^2=0.55$; North, $p<0.001$, $r^2=0.55$; South+, $p=0.001$, $r^2=0.44$, (C) full, $p<0.01$, $r^2=0.30$; North, $p=0.04$, $r^2=0.20$; South+, $p=0.01$, $r^2=0.30$, (D) Ice area, $p<0.01$, $r^2=0.33$; Ice days, $p=0.02$, $r^2=0.26$, (E) Ice area, $p<0.001$, $r^2=0.64$; Ice days, $p<0.001$, $r^2=0.63$.

1998 and 1999, possibly ushered in by a period of sustained La Niña conditions (Ross et al., 2008); the timing and sign of this change is consistent with our analysis.

PP, lagged by 2 years, was the best predictor of *E. superba* and *T. macrura* abundance in the multiple regression models, and was particularly strong for *E. superba*. *E. superba* growth and reproduction is dependent on food availability (Ross et al., 2000; Quetin and Ross, 2001; Atkinson et al., 2006). At a coastal station adjacent to Palmer Station, Saba et al. (2014) found years of positive chl *a* anomalies led to initiation of a strong krill cohort the following summer (i.e., 1-year lag), as evidenced by changes in size classes of krill in Adélie penguin diets. The 2-year lag we found for the WAP region as a whole is consistent with the first year of high PP initiating the cycle of 2 sequential good years of recruitment for Antarctic krill, cumulating in peak abundance 2 years later, as described above. Given that abundance of *T. macrura* (the other most abundant species of euphausiid) was also closely tied to anomalies in PP, there is obvious bottom-up control of the euphausiid population of the WAP, whether through direct feeding on phytoplankton, or on other, smaller consumers of phytoplankton.

E. crystallorophias abundance was most closely (and negatively) correlated to SAM (summer, 2-year lag), and highest 1–2 years following high ice conditions, particularly in the Far South. A positive SAM, associated with increased NW winds poleward and subsequent lower sea ice extent may lead to an early sea ice retreat and potentially warmer surface waters (Table 4). Our results are consistent with Ross et al. (2008) who found a positive correlation between abundance and distribution of *E. crystallorophias* and day of sea ice retreat (later). As *E. crystallorophias* is considered to be a coastal/neritic species that is associated with ice-covered regions (Ross et al., 2008; Guglielmo et al., 2009; Lee et al., 2013), our results are consistent with what is known about their ecology and association with colder water. However, as sea ice is decreasing in the South as well, and *E. crystallorophias* habitable range is projected to contract with warming (Mackey et al., 2012), we would predict a decline in their abundance in the future. The significant increase in the past decade of *E. crystallorophias* in the South may also be due to an increase in PP, or to more favorable timing of ice retreat and subsequent phytoplankton blooms with the food needs of the larvae in spring. Although PP did not surface as one of the most important predictors of *E. crystallorophias* abundance in our multiple regression model, there was a significant and positive relationship (no lag) between the two in the South+ ($p=0.02$, $r^2=0.30$).

4.2. Salps

Although there was no significant linear increase in *Salpa thompsoni* over time, like the pteropod *Limacina* (see below), *S. thompsoni* cycled between negative and positive anomalies in the North, but showed increasing positive anomalies in the South in the latter half of the time series. The latter is consistent with a shift in highest abundances from North to South in the earlier period, small-scale analysis of Ross et al. (2014). The prior winter SAM and MEI were both significant factors affecting salp abundance, and in the South salp abundances were negatively correlated with both sea ice area and ice

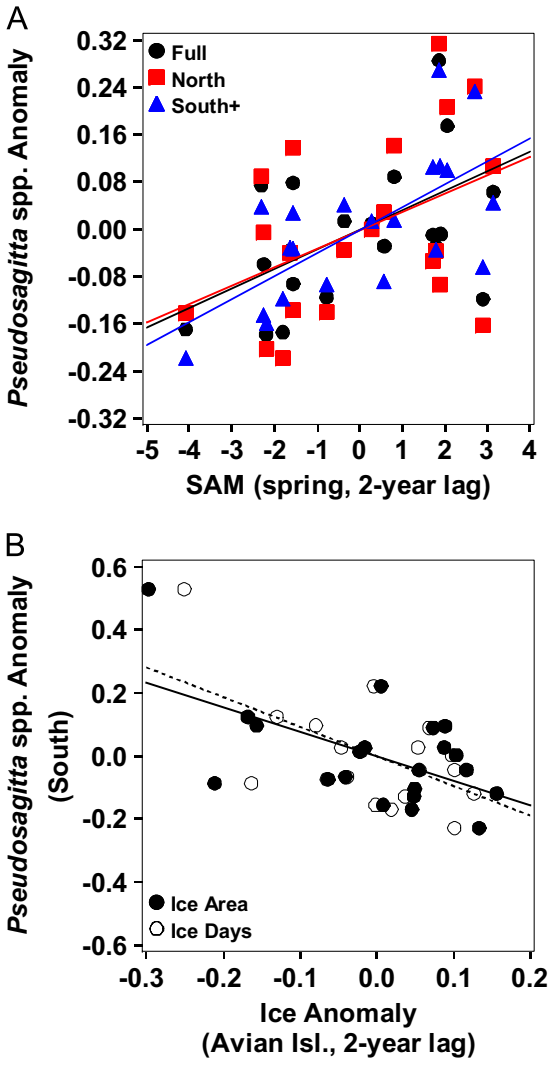

Fig. 12. Effect of Southern Annular Mode (SAM) and sea-ice on chaetognaths *Pseudosagitta* spp. (A) SAM spring index (2-year lag) vs. chaetognath *Pseudosagitta* spp. abundance, and (B) Ice area and Ice days (Avian Island, 2-year lag) vs. chaetognath *Pseudosagitta* spp. abundance for the South region. Data plotted are annual anomalies for each year of the time series (1993–2013) for indicated regions ('South+' is 'South' and 'Far South' regions combined; lines 300 to −100). In B, Avian Island is the 'South' ice sub-region, within 200 km south and west of Avian Island (see Section 2); solid and dashed regression lines correspond to ice area and days, respectively. Regressions were significant for all comparisons and lines are shown- statistics are as follows ($n=21$ for each): (A) full, $p=0.01$, $r^2=0.29$; North, $p=0.05$, $r^2=0.19$; South+, $p=0.001$, $r^2=0.44$, (B) Ice area, $p<0.01$, $r^2=0.33$; Ice days, $p<0.01$, $r^2=0.32$.

days. Positive SAM and negative MEI (La Niña) phases, leading to high salp abundance in our analysis, are both associated with decreased sea-level pressure in the WAP area and increased northerly winds (Yuan, 2004), which bring warmer, moister air to the WAP. The stronger northerly winds result in reduced sea ice extent and duration in the WAP region (Stammerjohn et al., 2008a) (Table 4). The higher abundance of *S. thompsoni* in ice-free conditions is predicted from what we know about their affinity for open, ice-free, warmer water conditions (e.g., Loeb et al., 1997; Pakhomov et al., 2002; Ross et al., 2008; and see below), which in the South may now provide an increasingly favorable, and expanding, environment. It is also possible that northerly winds resulting from positive SAM and negative MEI conditions in winter alter surface circulation, bringing the seed population of salps (solitary stage) in slope waters closer to the shelf, such that the following January (during our sampling) there will be a salp bloom at the shelf break, or over the shelf. The negative correlation we found between MEI and salp abundance is the opposite trend reported by Loeb and Santora (2012) for salps in the AMLR study located north of the PAL LTER region, who found *S. thompsoni* abundance was positively correlated with the fall and winter Niño 3.4 Index (which in sign closely tracks the MEI; data not shown). They suggest in this region that conditions following reversal from La Niña to El Niño (negative to positive MEI) are associated with increased salp production and massive bloom formation (Loeb and Santora, 2012).

4.3. Relationship between *E. superba* and *S. thompsoni* distribution and abundance

We found a pronounced inverse relationship between *E. superba* and *S. thompsoni* in both space and time when abundance of either species was at its highest, but at lower densities these species were more likely to overlap in their distribution. The spatial separation of Antarctic krill and salps throughout much of the Southern Ocean has been widely documented, with the Antarctic Peninsula region being a notable exception where the two species are considered to co-occur, at least in summer (Pakhomov et al., 2002; Ross et al., 2008). On large spatial scales (> 100 km) separation of the two species may be related to water mass distribution (Pakhomov et al., 2002), and overlap in distribution of Antarctic krill and salps in the WAP explained by the complex mixing of different water masses characteristic of this region (Pakhomov et al., 2002; Dinniman and Klinck, 2004; Murphy et al., 2013). Another, not mutually exclusive, explanation is competitive exclusion, whereby salps consume krill eggs or larvae, or one species outcompetes the other for food (e.g., salps are more efficient consumers at lower prey densities and on smaller phytoplankton sizes than krill, and visa versa) (Pakhomov et al., 2002). Ultimately, warming is expected to lead to an increase in the degree of spatial separation between Antarctic krill and salps (Atkinson et al., 2004).

In addition, large temporal differences in relative abundance of Antarctic krill and salps have been attributed to interannual differences in water temperature and sea-ice cover – with warmer, low sea-ice cover (open water) conditions favoring salp blooms, and colder years with high sea-ice cover favoring krill recruitment the following summer (Siegel and Loeb, 1995; Loeb et al., 1997). While we did not find an overall significant relationship for the time series between annual anomalies of sea ice parameters or temperature vs. krill, or salps, we did find that high spring SST anomalies in some years (e.g., 2009 and 2010 in the North, Fig. 9c) were followed by anomalously high salp abundance in January (e.g., 2010 and 2011, Fig. 4a). In January, 2011 temperatures at some stations reached 5 °C in surface waters, and salps were distributed across the entire grid. Salp abundance anomalies also switched from negative to positive in 2009, following the lowest ice year – 2008 (Fig. 9a and b). Conversely, years with winters of relatively higher ice extent and duration (2011 and 2012, Fig. 9a and b) were followed by years of anomalously high summer *E. superba* abundance (2012 and 2013). Ross et al. (2008) also found WAP salp abundance (1993–2004) was positively correlated with the timing of sea ice advance and negatively with duration of ice cover.

Marked spatial or interannual differences in the relative abundance of these species have potential consequences for energy flow through the WAP food web and for export of carbon to depth. Total macrozooplankton community grazing rates during summer in the WAP were greatest in the slope waters, where *S. thompsoni* occurred in dense blooms (Bernard et al., 2012) suggesting high energy flow through salps in this region. Grazing impact by krill (*E. superba*), however, is highest in the coastal region (Ross et al., 1998; Bernard et al., 2012). As a prey item for higher trophic levels, the chemical energy content of krill (e.g., proteins 65% and lipids 14% of dry weight) far exceeds that of salps (e.g., proteins 5% and lipids 6% of dry weight; Dubischar et al., 2006). Thus, under a low krill, salp-dominated

Table 4
Putative affects of climate indices and environmental parameters on WAP macrozooplankton species abundance as indicated by results of this study. Note that affect on each species listed can be result of a single, or combination of indices and environmental parameters listed. Index, climate index or environmental parameter; SLP, sea level pressure; PP, primary production; Chl *a*, chlorophyll *a*.

Index	Sign	Predicted impact	Affect on species abundance
SAM	+	Negative SLP anomaly to west of Antarctic Peninsula region, cyclonic (clockwise flowing)	–*E. crystallorophias*
MEI	–(La Niña)	atmospheric circulation, increased NW and warmer winds poleward. Unfavorable conditions	+*S. thompsoni*
Ice	–	for sea ice: lower sea ice extent,	+*L. helicina*
SST	+	early sea ice retreat, potentially warmer surface waters	+*Pseudosagitta* spp.
			+*Tomopteris* spp.
SAM	–	Positive SLP anomaly to west of Antarctic Peninsula region, anticyclonic (counterclockwise flowing)	+ *E. crystallorophias*
MEI	+(El Niño)	atmospheric circulation, cold southerly winds over the WAP. Favorable conditions for sea ice:	−*S. thompsoni*
Ice	+	Greater sea ice extent, later sea ice retreat, potentially colder surface waters	−*L. helicina*
SST	–		−*Pseudosagitta* spp.
			−*Tomopteris* spp.
PP & Chl *a*	+	Increased food, bottom-up control	+*E. superba*
			+*T. macrura*

scenario, predators (fish, penguins and other sea birds, seals, and whales) may be unable to meet their energetic requirements, leading to a decrease in some predator populations (although abundant mesozooplankton such as copepods, e.g., Ward et al. (2012), which are consumed by fish may be an alternate trophic pathway). In addition, zooplankton fecal pellets, mostly from krill, constitute the dominant proportion of total export flux (67%, in summer) over the continental shelf of the northern WAP (Gleiber et al., 2012). Regional or temporal increases in the abundance of salps – indiscriminate filter feeders which, unlike krill, are able to feed on small-celled phytoplankton – could lead to increased export, due to their high feeding rates and production of very large, fast-sinking fecal pellets ($\sim$700 m d^{-1}; Phillips et al., 2009), or to more sporadic export events, due to the ephemeral nature of salp blooms (Gleiber et al., 2012).

4.4. *Limacina pteropods and the ice-climate link*

The shelled pteropod *Limacina helicina antarctica* is an abundant and often major component of the macrozooplankton community along the WAP (Ross et al., 2008; Loeb and Santora, 2013). Recent studies of *Limacina* have been stimulated by concerns about the deleterious effects of elevated seawater carbon dioxide levels and resulting ocean acidification (Doney et al., 2009). Such effects on pteropods include dissolution of their aragonite shells (Orr et al., 2005; Roberts et al. 2008; Bednaršek et al., 2012a), and suppression of their metabolism (Seibel et al., 2012). There is now evidence for in situ dissolution of pteropod shells in parts of the water column northeast of the Antarctic Peninsula that are undersaturated in aragonite (Bednaršek et al., 2012a).

We thus hypothesized a potential decreasing trend in *Limacina helicina* in the PAL study region, but rather found an alternation between high and low abundance anomalies in the North and an increase in positive anomalies later in the time series in the South. This is because of all the major taxa analyzed, *L. helicina* was the taxa most closely tied to ENSO climate indices, sea ice, and SST. The strong negative correlation between *L. helicina* abundance and the MEI is consistent with that seen for *L. helicina* and the predatory, unshelled pteropod *Spongiobranchaea australis* in a time-series analysis (1994–2009) of pteropods in the WAP north of our study area, where significant increases in their abundance after 1998 were associated with La Niña conditions (i.e., negative ENSO indices) (Loeb and Santora, 2013). Ross et al. (2008) also show a change in *L. helicina* in our study region of the WAP after 1998. This is clearly seen in our analysis as well, where a large negative anomaly in 1998 coinciding with the strong 1997/1998 El Niño event is followed by six years of positive anomalies.

We also found increasing *L. helicina* abundance correlated to decreasing sea ice area and ice days, especially in the South, and to increasing SST throughout the grid. We posit that similar to salps, the increasingly ice-free, warmer, and productive waters in the South have provided a favorable, and expanding, environment for *L. helicina* growth. *L. helicina* abundance has been linked to phytoplankton production in the Ross Sea (Seibel and Dierssen, 2003), and *L. helicina* is an important grazer in the WAP that can at times account for a larger percentage of macrozooplankton community grazing of PP than krill (Bernard et al., 2012). Thus, an increasing amount of energy in the WAP food web is expected to be processed through *L. helicina* if this trend in increasing abundance continues.

4.5. *Increasing carnivorous gelatinous zooplankton, and amphipods*

Carnivorous gelatinous zooplankton (*Pseudosagitta* spp. chaetognaths, and *Tomopteris* sp. polychaete worms) generally increased in abundance over the time series, and their abundances were significantly correlated with each other. There was also an indication of an increase in amphipods other than *Themisto gaudichaudii* over the last decade. While these increases could have resulted from increased PP (bottom-up control) as suggested by our analyses, the effect is a potential increase in top-down control on the WAP food web over time, as noted in previous studies on shorter, seasonal time scales. For example, in the Lazarev Sea the epipelagic food web shifted from bottom-up control in summer to top-down control in winter, due to the high abundance (44–60% of total) and biomass (39–58%) of carnivorous macrozooplankton, increased winter carnivory by omnivorous species, and lower winter PP (Hunt et al., 2011). Increased knowledge of the ecology and energy flow through carnivorous zooplankton in the WAP will be key to interpreting the causes and consequences of these changes.

The species diversity of carnivorous macrozooplankton in the epipelagic zone of the Southern Ocean is relatively low (Pakhomov and Froneman, 1999), and in the WAP only a few species generally dominated the carnivorous taxa in any given net tow. Chaetognaths are one of the most abundant predators, and amongst all carnivore groups were the most important consumers of secondary production along a transect of the Atlantic sector of the Southern Ocean from the Antarctic continent to Cape Town, South Africa (Pakhomov et al., 1999). Chaetognaths consumed up to 5% of copepod standing stock and 100% of copepod production per day in the subantarctic (Froneman and Pakhomov, 1998), and $<1\%$ of copepod standing stock in the WAP (Øresland, 1990) (due to low secondary production of copepods and other prey, chaetognaths would consume relatively more production than standing stock). There are limited data reported in the WAP for the other gelatinous carnivore we considered,

Tomopteris spp. polychaetes. Mean density of *Tomopteris* spp. in our time series (0.5 ind. 1000 m^{-3}) was intermediate compared to previous studies– lower than at South Georgia in summer and winter (9 and 17 ind. 1000 m^{-3}, respectively, Ward, 1989), and higher than in Marguerite Bay in autumn and winter (0.03 and 0.04 ind. 1000 m^{-3}, respectively, Parker et al., 2011). Like salps and pteropods, both large chaetognath and polychaete abundance was significantly influenced by sea ice, with higher abundance following lower ice conditions the year prior. Thus trends in decreasing sea ice are predicted to be favorable for these species, at least in the near term.

The amphipod *T. gaudichaudii* consumes a variety of other zooplankton, including copepods, chaetognaths, and the pteropod *L. helicina* (Watts and Tarling, 2012; Murphy et al., 2013), and is reported to be capable of consuming 100% of the total zooplankton production near South Georgia in summer (Watts and Tarling, 2012). This species is most abundant in the far northern WAP, and is itself an important prey item for fish, penguins, and other sea birds (Watts and Tarling, 2012; Murphy et al., 2013), becoming an important prey item for penguins near South Georgia, especially during years of low krill abundance (Murphy et al., 2013). We were not able to detect any cycles or long-term trends in *T. gaudichaudii* abundance. However, other (mostly hyperiid) amphipods increased over the time series, and their abundance was influenced by the MEI and SAM. Some of these hyperiid species are parasitic or otherwise associated with gelatinous zooplankton including salps (e.g., Madin and Harbison, 1977), or like *T. gaudichaudii*, may consume *L. helicina* (Hunt et al., 2008). Changes in abundance of some of these other species may be influencing amphipod abundance, as suggested by the positive correlation between 'other' amphipods and *L. helicina*.

5. Conclusion

One of our predictions was that the north–south climate gradient along the WAP affects zooplankton abundance over space and time, and for several species we did find increases over time that were significant in one region but not another. For example, *T. macrura* increased in the North, and *E. crystallorphias* in the South. These long-term trends may ultimately be a result of increasing PP across the grid, especially in the South. We note that both our 'North' and 'South' subregions constitute the 'south' subregion in the satellite data analysis by Montes-Hugo et al. (2009), for which an increasing trend in chl *a* over time was also found. Some of the carnivores also increased (e.g., *Tomopteris* spp., large chaetognaths, 'other' amphipods). One alternate interpretation of increasing trends in abundance is that due to warming, ice is retreating earlier, causing phytoplankton blooms to occur earlier in the season, leading to a progressively earlier increase in zooplankton abundance. Thus, the increase we detect in January/February over 20 years, could reflect a change in zooplankton phenology (the timing of life cycle events, Edwards and Richardson, 2004), rather than an actual long-term increase in abundance. Since we do not sample the entire grid in the early spring we cannot rule out this alternative explanation. However, at least on the north coast near Palmer Station where seasonal sampling (October to March) is performed (Saba et al., 2014), there is no detectable directional long-term trend in the timing of phytoplankton blooms (as determined by chl *a*) (Schofield et al. unpublished). Another consideration is that in the north where there is now barely an ice season, other environmental controls on phytoplankton (such as the effect of wind on mixed layer depth) dominate, in turn affecting zooplankton. Regardless of the ultimate reason for these observed trends, changes in zooplankton distribution in time and space could lead to increased trophic mismatches, and perhaps even species loss.

Clearly a host of environmental factors explain temporal variation in abundance of WAP macrozooplankton, with some species more closely tied to PP (*E. superba*, *T. macrura*), some to climate oscillations such as ENSO (*L. helicina*) and SAM (e.g., *S. thompsoni*, *E. crystallorophias*), and some to ice (high ice conditions – *E. crystallorophias*, lower ice- *S. thompsoni*, *L. helicina*, *Pseudosagitta* spp., and *Tomopteris* spp.). Interestingly, we found that the time elapsed between the state of a given environmental parameter and the effect on taxon abundance, ranged from coincident (during the same month) to a 1- or 2-year delay. Loeb and Santora (2012) found similar results 'supporting the role of multi-year atmospheric-oceanic processes', associated with ENSO, affecting the population dynamics of *S. thompsoni*. In addition, we tended to find no, or shorter, lags for salps and pteropods, and longer lags for longer-lived krill (e.g., 2-year lag in the effect of PP), supporting the assertion of Ross et al. (2008) that the mechanisms driving spatial and temporal distribution of shorter-lived, more oceanic species (e.g., salps and pteropods) are less complex and more direct than for longer-lived euphausiids (although recent studies now indicate *Limacina helicina* can live for 3 years or more, Bednaršek et al., 2012b). Ultimately, both the long-term changes and sub-decadal cycles in WAP macrozooplankton community composition that we observe could affect energy transfer to higher trophic levels, and alter biogeochemical cycling in this seasonally productive ecosystem.

Acknowledgments

We thank the Captain, officers, and crew of the MV *Polar Duke* and ARSV *Laurence M. Gould*, and Raytheon Polar Services and Lockheed Martin personnel for their scientific and logistical support. We are grateful to the many student volunteers that assisted during the PAL LTER cruises and in the laboratory. We thank Doug Martinson and Rich Iannuzzi for consult on sea surface temperature data, Grace Saba for advice with climate index analyses, Josh Stone for assistance with figure preparation, and Hugh Ducklow for helpful discussions and his leadership of the PAL LTER. We also thank B. Prezelin, M. Vernet and R. Smith for historical PP and Chl *a* data used in our analyses. This research was supported by the National Science Foundation Antarctic Organisms and Ecosystems Program (OPP-0823101). This is contribution number 3450 from the Virginia Institute of Marine Science.

Appendix A. Supplementary materials

Supplementary data associated with this article can be found in the online version at http://dx.doi.org/10.1016/j.dsr.2015.02.009.

References

Atkinson, A., Siegel, V., Pakhomov, E., Rothery, P., 2004. Long-term decline in krill stock and increase in salps within the Southern Ocean. Nature 432, 100–103.
Atkinson, A., Shreeve, R.S., Hirst, A.G., Rothery, P., Tarling, G.A., Pond, D.W., Korb, R.E., Murphy, E.J., Watkins, J.L., 2006. Natural growth rates in Antarctic krill (*Euphausia superba*): II. Predictive models based on food, temperature, body length, sex, and maturity stage. Limnol. Oceanogr. 51 (2), 973–987.
Atkinson, A., Siegel, V., Pakhomov, E.A., Rothery, P., Loeb, V., Ross, R.M., Quetin, L.B., Schmidt, K., Fretwell, P., Murphy, E.J., Tarling, G.A., Feming, A.H., 2008. Oceanic circumpolar habitats of Antarctic krill. Mar. Ecol. Prog. Ser. 362, 1–23.
Atkinson, A., Siegel, V., Pakhomov, E.A., Jessopp, M.J., Loeb, V., 2009. A re-appraisal of the total biomass and annual production of Antarctic krill. Deep-Sea Res. I 56 (5), 727–740.
Bednaršek, N., Tarling, G.A., Bakker, D.C.E., Fielding, S., Jones, E.M., Venables, H.J., Ward, P., Kuzirian, A., Leze, B., Feely, R.A., Murphy, E.J., 2012a. Extensive dissolution of live pteropods in the Southern Ocean. Nat. Geosci. 5 (12), 881–885.
Bednaršek, N., Tarling, G.A., Fielding, S., Bakker, D.C.E., 2012b. Population dynamics and biogeochemical significance of *Limacina helicina antarctica* in the Scotia Sea (Southern Ocean). Deep-Sea Res. II 59, 105–116.
Belsley, D.A., Kuh, E., Welsch, R.E., 1980. Regression Diagnostics. John Wiley & Sons, Inc., Hoboken, NJ p. 292.
Bernard, K.S., Steinberg, D.K., Schofield, O.M.E., 2012. Summertime grazing impact of the dominant macrozooplankton off the Western Antarctic Peninsula. Deep-Sea Res. I 62, 111–122.
Daly, K.L., Macaulay, M.C., 1988. Abundance and distribution of krill in the ice edge zone of the Weddell Sea, Austral Spring 1983. Deep-Sea Res. 35 (1), 21–41.

Dinniman, M.S., Klinck, J.M., 2004. A model study of circulation and cross-shelf exchange on the west Antarctic Peninsula continental shelf. Deep-Sea Res. II 51 (17–19), 2003–2022.
Doney, S.C., Fabry, V.J., Feely, R.A., Kleypas, J.A., 2009. Ocean Acidification: the other CO_2 problem. Annu. Rev. Mar. Sci. 1, 169–192.
Dubischar, C., Pakhomov, E., Bathmann, U., 2006. The tunicate *Salpa thompsoni* ecology in the Southern Ocean. II. Proximate and elemental composition. Mar. Biol. 149 (3), 625–632.
Ducklow, H.W., Baker, K., Martinson, D.G., Quetin, L.B., Ross, R.M., Smith, R.C., Stammerjohn, S.E., Vernet, M., Fraser, W., 2007. Marine pelagic ecosystems: the West Antarctic Peninsula. Philos. Trans. R. Soc. B Biol. Sci. 362 (1477), 67–94.
Ducklow, H.W., Clarke, A., Dickhut, R., Doney, S.C., Geisz, H., Huang, K., Martinson, D.G., Meredith, M.P., Moeller, H.V., Montes-Hugo, M., Schofield, O., Stammerjohn, S.E., Steinberg, D.K., Fraser, W., 2012a. The marine system of the Western Antarctic Peninsula. In: Rogers, A.D., Johnston, N.M., Murphy, E.J., Clarke, A. (Eds.), Antarctic Ecosystems: An Extreme Environment in a Changing World. Blackwell, London, pp. 121–159.
Ducklow, H.W., Schofield, O., Vernet, M., Stammerjohn, S., Erickson, M., 2012b. Multiscale control of bacterial production by phytoplankton dynamics and sea ice along the western Antarctic Peninsula: a regional and decadal investigation. J. Mar. Syst. 98–99, 26–39.
Ducklow, H.W., Fraser, W.R., Meredith, M.P., Stammerjohn, S.E., Doney, S.C., Martinson, D.G., Sailley, S.F., Schofield, O.M., Steinberg, D.K., Venables, H.J., Amsler, C.D., 2013. West Antarctic Peninsula: an ice-dependent coastal marine ecosystem in transition. Oceanography 26 (3), 190–203.
Edwards, M., Richardson, A.J., 2004. Impact of climate change on marine pelagic phenology and trophic mismatch. Nature 430 (7002), 881–884.
Flores, H., Atkinson, A., Kawaguchi, S., Krafft, B.A., Milinevsky, G., Nicol, S., Reiss, C., Tarling, G.A., Werner, R., Bravo, E., Cirelli, V., Cuzin-Roudy, J., Fielding, S., van Franeker, J., Groeneveld, J.J., Haraldsson, M., Lombana, A., Marschoff, E., Meyer, B., Pakhomov, E.A., Van de Putte, A.P., Rombolá, E., Schmidt, K., Siegel, V., Teschke, M., Tonkes, H., Toullec, J.Y., Trathan, P.N., Tremblay, N., Werner, T., 2012. Impact of climate change on Antarctic krill. Mar. Ecol. Prog. Ser. 458, 1–19.
Fraser, W.R., Hofmann, E.E., 2003. A predator's perspective on causal links between climate change, physical forcing and ecosystem response. Mar. Ecol. Prog. Ser. 265, 1–15.
Froneman, P.W., Pakhomov, E.A., 1998. Trophic importance of the chaetognaths *Eukrohnia hamata* and *Sagitta gazellae* in the pelagic system of the Prince Edward Islands (Southern Ocean). Pol. Biol. 19 (4), 242–249.
Fuller, W.A, 1996. Introduction to Statistical Time Series. John Wiley & Sons, New York, 698 pp.
Garibotti, I.A., Vernet, M., Ferrario, M.E., Smith, R.C., Ross, R.M., Quetin, L.B., 2003. Phytoplankton spatial distribution patterns along the western Antarctic Peninsula (Southern Ocean). Mar. Ecol. Prog. Ser. 261, 21–39.
Garzio, L.M., Steinberg, D.K., 2013. Microzooplankton community composition along the Western Antarctic Peninsula. Deep-Sea Res. I 77, 36–49.
Gleiber, M.R., Steinberg, D.K., Ducklow, H.W., 2012. Time series of vertical flux of zooplankton fecal pellets on the continental shelf of the western Antarctic Peninsula. Mar. Ecol. Prog. Ser. 471, 23–36.
Guglielmo, L., Donato, P., Zagami, G., Granata, A., 2009. Spatio-temporal distribution and abundance of *Euphausia crystallorophias* in Terra Nova Bay (Ross Sea, Antarctica) during austral summer. Pol. Biol. 32 (3), 347–367.
Haraldsson, M., Siegel, V., 2014. Seasonal distribution and life history of *Thysanoessa macrura* (Euphausiacea, Crustacea) in high latitude waters of the Lazarev Sea, Antarctica. Mar. Ecol. Prog. Ser. 495, 105–118.
Holland, P.R., Kwok, R., 2012. Wind-driven trends in Antarctic sea-ice drift. Nat. Geosci. 5 (12), 872–875.
Hunt, B.P.V., Pakhomov, E.A., Hosie, G.W., Siegel, V., Ward, P., Bernard, K., 2008. Pteropods in Southern Ocean ecosystems. Prog. Oceanogr. 78 (3), 193–221.
Hunt, B.P.V., Pakhomov, E.A., Siegel, V., Strass, V., Cisewski, B., Bathmann, U., 2011. The seasonal cycle of the Lazarev Sea macrozooplankton community and a potential shift to top-down trophic control in winter. Deep-Sea Res. II 58 (13–16), 1662–1676.
Hurrell, J.W., 1995. Decadal trends in the North-Atlantic oscillation – regional temperatures and precipitation. Science 269 (5224), 676–679.
Lee, D.B., Choi, K.H., Ha, H.K., Yang, E.J., Lee, S.H., Lee, S., Shin, H.C., 2013. Mesozooplankton distribution patterns and grazing impacts of copepods and *Euphausia crystallorophias* in the Amundsen Sea, West Antarctica, during austral summer. Pol. Biol. 36 (8), 1215–1230.
Loeb, V., Siegel, V., Holm-Hansen, O., Hewitt, R., Fraser, W., Trivelpiece, W., Trivelpiece, S., 1997. Effects of sea-ice extent and krill or salp dominance on the Antarctic food web. Nature 387 (6636), 897–900.
Loeb, V., 2007. Environmental variability and the Antarctic marine ecosystem. Impact Environ. Var. Ecol. Syst. 2, 197–225.
Loeb, V.J., Hofmann, E.E., Klinck, J.M., Holm-Hansen, O., White, W.B., 2009. ENSO and variability of the Antarctic Peninsula pelagic marine ecosystem. Antarct. Sci. 21 (2), 135–148.
Loeb, V.J., Santora, J.A., 2012. Population dynamics of *Salpa thompsoni* near the Antarctic Peninsula: growth rates and interannual variations in reproductive activity (1993–2009). Prog. Oceanogr. 96 (1), 93–107.
Loeb, V.J., Santora, J.A., 2013. Pteropods and climate off the Antarctic Peninsula. Prog. Oceanogr. 116, 31–48.
Madin, L.P., Harbison, G.R., 1977. Associations of Amphipoda-Hyperiidea with Gelatinous-Zooplankton.1. Associations with Salpidae. Deep-Sea Res. 24 (5), 449–463.
Mackey, A.P., Atkinson, A., Hill, S.L., Ward, P., Cunningham, N.J., Johnston, N.M., Murphy, E.J., 2012. Antarctic macrozooplankton of the southwest Atlantic sector and Bellingshausen Sea: baseline historical distributions (*Discovery Investigations*, 1928–1935) related to temperature and food, with projections for subsequent ocean warming. Deep-Sea Res. II 59–60, 130–146.
Martinson, D.G., Stammerjohn, S.E., Iannuzzi, R.A., Smith, R.C., Vernet, M., 2008. Western Antarctic Peninsula physical oceanography and spatio-temporal variability. Deep-Sea Res. II 55 (18–19), 1964–1987.
Meeus, J., 1998. Astronomical Algorithms, second edition Willmann-Bell, Inc., Richmond, VA, 477 pp.
Meredith, M.P., King, J.C., 2005. Rapid climate change in the ocean west of the Antarctic Peninsula during the second half of the 20th century. Geophys. Res. Lett. 32 (19), L19604.
Montes-Hugo, M., Doney, S.C., Ducklow, H.W., Fraser, W., Martinson, D., Stammerjohn, S.E., Schofield, O., 2009. Recent changes in phytoplankton communities associated with rapid regional climate change along the Western Antarctic Peninsula. Science 323, 1470–1473.
Montes-Hugo, M., Sweeney, C., Doney, S.C., Ducklow, H., Frouin, R., Martinson, D.G., Stammerjohn, S., Schofield, O., 2010. Seasonal forcing of summer dissolved inorganic carbon and chlorophyll a on the western shelf of the Antarctic Peninsula. J. Geophys. Res.-Oceans 115, C03024, 10.1029/2009JC005267.
Murphy, E.J., Hofmann, E.E., Watkins, J.L., Johnston, N.M., Pinones, A., Ballerini, T., Hill, S.L., Trathan, P.N., Tarling, G.A., Cavanagh, R.A., Young, E.F., Thorpe, S.E., Fretwell, P., 2013. Comparison of the structure and function of Southern Ocean regional ecosystems: the Antarctic Peninsula and South Georgia. J. Mar. Syst. 109, 22–42.
Neter, J., Kutner, M.H., Nachtsheim, C.J., Wasserman, W., 1996. Applied Linear Statistical Models, fourth edition Irwin, Chicago p. 1408.
Nowacek, D.P., Friedlaender, A.S., Halpin, P.N., Hazen, E.L., Johnston, D.W., Read, A.J., Espinasse, B., Zhou, M., Zhu, Y.W., 2011. Super-aggregations of krill and Humpback Whales in Wilhelmina Bay, Antarctic Peninsula. PloS One 6 (4).
O'Brien, T.D., López-Urrutia, A., Wiebe, P.H., Hay, S., 2008. ICES Zooplankton Status Report 2006/2007. 168 pp.
Øresland, V., 1990. Feeding and predation impact of the chaetognath Eukrohnia hamata in Gerlache Strait, Antarctic Peninsula. Mar. Ecol. Prog. Ser. 63, 201–209.
Orr, J.C., Fabry, V.J., Aumont, O., Bopp, L., Doney, S.C., Feely, R.A., Gnanadesikan, A., Gruber, N., Ishida, A., Joos, F., Key, R.M., Lindsay, K., Maier-Reimer, E., Matear, R., Monfray, P., Mouchet, A., Najjar, R.G., Plattner, G.K., Rodgers, K.B., Sabine, C.L., Sarmiento, J.L., Schlitzer, R., Slater, R.D., Totterdell, I.J., Weirig, M.F., Yamanaka, Y., Yool, A., 2005. Anthropogenic ocean acidification over the twenty-first century and its impact on calcifying organisms. Nature 437 (7059), 681–686.
Pakhomov, E.A., Perissinotto, R., Froneman, P.W., 1999. Predation impact of carnivorous macrozooplankton and micronekton in the Atlantic sector of the Southern Ocean. J. Mar. Sys. 19, 47–64.
Pakhomov, E.A., Froneman, P.W., 1999. Macroplankton/micronekton dynamics in the vicinity of the Prince Edward Islands (Southern Ocean). Mar. Biol. 134 (3), 501–515.
Pakhomov, E.A., Froneman, P.W., Perissinotto, R., 2002. Salp/krill interactions in the Southern Ocean: spatial segregation and implications for the carbon flux. Deep-Sea Res. II 49, 1881–1907.
Parker, M.L., Donnelly, J., Torres, J.J., 2011. Invertebrate micronekton and macrozooplankton in the Marguerite Bay region of the Western Antarctic Peninsula. Deep-Sea Res. II 58 (13–16), 1580–1598.
Phillips, B., Kremer, P., Madin, L.P., 2009. Defecation by *Salpa thompsoni* and its contribution to vertical flux in the Sothern Ocean. Mar. Biol. 156, 455–467.
Roberts, D., Howard, W.R., Moy, A.D., Roberts, J.L., Trull, T.W., Bray, S.G., Hopcroft, R. R., 2008. Interannual variability of pteropod shell weights in the high-CO_2 Southern Ocean. Biogeosciences Discuss. 5, 4453–4480.
Quetin, L.B., Ross, R.M., 2001. Environmental variability and its impact on the reproductive cycle of Antarctic krill. Am. Zool. 41 (1), 74–89.
Quetin, L.B., Ross, R.M., 2003. Episodic recruitment in Antarctic krill *Euphausia superba* in the Palmer LTER study region. Mar. Ecol. Prog. Ser. 259, 185–200.
Renwick, J.A., 2002. Southern hemisphere circulation and relations with sea ice and sea surface temperature. J. Clim. 15 (21), 3058–3068.
Reynolds, R.W., Rayner, N.A., Smith, T.M., Stokes, D.C., Wang, W., 2002. An improved in situ and satellite SST analysis for climate. J. Clim. 15, 1609–1625.
Ross, R.M., Quetin, L.B., Haberman, K.L., 1998. Interannual and seasonal variability in short-term grazing impact of *Euphausia superba* in nearshore and offshore waters west of the Antarctic Peninsula. J. Mar. Syst. 17 (1–4), 261–273.
Ross, R.M., Quetin, L.B., Baker, K.S., Vernet, M., Smith, R.C., 2000. Growth limitation in young *Euphausia superba* under field conditions. Limnol. Oceanogr. 45 (1), 31–43.
Ross, R.M., Quetin, L.B., Martinson, D.G., Iannuzzi, R.A., Stammerjohn, S.E., Smith, R. C., 2008. Palmer LTER: patterns of distribution of five dominant zooplankton species in the epipelagic zone west of the Antarctic Peninsula, 1993–2004. Deep-Sea Res. II 55, 2086–2105.
Ross, R.M., Quetin, L.B., Newberger, T., Shaw, C.T., Jones, J.L., Oakes, S.A., Moore, K.J., 2014. Trends, cycles, interannual variability for three pelagic species west of the Antarctic Peninsula 1993–2008. Mar. Ecol. Prog. Ser. 515, 11–32.
Ruck, K.E., Steinberg, D.K., Canuel, E.A., 2014. Regional differences in quality of krill and fish as prey along the Western Antarctic Peninsula. Mar. Ecol. Prog. Ser. 509, 39–55.
Saba, G.K., Fraser, W.R., Saba, V.S., Iannuzzi, R.A., Coleman, K.C., Doney, S.C., Ducklow, H.W., Martinson, D.G., Miles, T.N., Patterson-Fraser, D.L., Stammerjohn, S.E., Steinberg, D.K., Schofield, O.M., 2014. Winter and spring controls on the summer food web of the coastal West Antarctic Peninsula. Nat. Commun. 5 4318, 10.1038/ncomms5318.

Saba, G.K., Schofield, O., Torres, J.J., Ombres, E.H., Steinberg, D.K., 2012. Increased feeding and nutrient excretion of adult Antarctic Krill, *Euphausia superba*, exposed to enhanced carbon dioxide (CO_2). PloS One 7 (12), e52224, 10.1371/journal.pone.0052224.

Sailley, S.F., Vogt, M., Doney, S.C., Aita, M.N., Bopp, L., Buitenhuis, E.T., Hashioka, T., Lima, I., Le Quere, C., Yamanaka, Y., 2013. Comparing food web structures and dynamics across a suite of global marine ecosystem models. Ecol. Model. 261, 43–57.

Seibel, B.A., Dierssen, H.M., 2003. Cascading trophic impacts of reduced biomass in the Ross Sea, Antarctica: just the tip of the iceberg?, Biol. Bull. 205 (2), 93–97.

Seibel, B.A., Maas, A.E., Dierssen, H.M., 2012. Energetic plasticity underlies a variable response to ocean acidification in the Pteropod, *Limacina helicina antarctica*. PloS One 7 (4), e30464, http://dx.doi.org/10.1371/journal.pone.0030464.

Siegel, V., Loeb, V., 1995. Recruitment of Antarctic krill *Euphausia superba* and possible causes for its variability. Mar. Ecol. Prog. Ser. 123, 45–56.

Siegel, V., 2005. Distribution and population dynamics of *Euphausia superba*: summary of recent findings. Pol. Biol. 29 (1), 1–22.

Smetacek, V., Nicol, S., 2005. Polar ocean ecosystems in a changing world. Nature 437 (7057), 362–368.

Smith, R.C., Ainley, D., Baker, K., Domack, E., Emslie, S., Fraser, B., Kennett, J., Leventer, A., Mosley-Thompson, E., Stammerjohn, S., Vernet, M., 1999. Marine ecosystem sensitivity to climate change. BioScience 49 (5), 393.

Stammerjohn, S.E., Martinson, D.G., Smith, R.C., Iannuzzi, R.A., 2008a. Sea ice in the western Antarctic Peninsula region: spatio-temporal variability from ecological and climate change perspectives. Deep-Sea Res. II 55, 2041–2058.

Stammerjohn, S.E., Martinson, D.G., Smith, R.C., Yuan, X., Rind, D., 2008b. Trends in Antarctic annual sea ice retreat and advance and their relation to El Niño and Southern Annular Mode variability. J. Geophys. Res. 113, C03S90.

Stammerjohn, S., Massom, R., Rind, D., Martinson, D., 2012. Regions of rapid sea ice change: an inter-hemispheric seasonal comparison. Geophys. Res. Lett. 39 (6), L06501.

Vaughan, D.G., Marshall, G.J., Connolley, W.M., Parkinson, C., Mulvaney, R., Hodgson, D.A., King, J.C., Pudsey, C.J., Turner, J., 2003. Recent rapid regional climate warming on the Antarctic Peninsula. Clim. Change 60 (3), 243–274.

Vernet, M., Martinson, D., Iannuzzi, R., Stammerjohn, S., Kozlowski, W., Sines, K., Smith, R., Garibotti, I., 2008. Primary production within the sea-ice zone west of the Antarctic Peninsula: I-Sea ice, summer mixed layer, and irradiance. Deep-Sea Res. II 55 (18–19), 2068–2085.

Ward, P., 1989. The distribution of zooplankton in an Antarctic fjord at South Georgia during summer and winter. Antarct. Sci. 1 (02), 141–150.

Ward, P., Atkinson, A., Tarling, G., 2012. Mesozooplankton community structure and variability in the Scotia Sea: a seasonal comparison. Deep-Sea Res. II 59–60, 78–92.

Waters, K.J., Smith, R.C., 1992. Palmer LTER: a sampling grid for the Palmer LTER program. Antarct. J. U. S. 27, 236–239.

Watts, J., Tarling, G.A., 2012. Population dynamics and production of *Themisto gaudichaudii* (Amphipoda, Hyperiidae) at South Georgia, Antarctica. Deep-Sea Res. II 59, 117–129.

Yuan, X., 2004. ENSO-related impacts on Antarctic sea ice: a synthesis of phenomenon and mechanisms. Antarct. Sci. 16 (4), 415–425.

Zhang, T., Osterkamp, T.E., Stamnes, K., 1997. Effects of climate on the active layer and permafrost on the north slope of Alaska, USA. Permafrost Periglac. Process. 8 (1), 45–67.